Supplementary Information File

Human aneuploid cells depend on the RAF/MEK/ERK pathway for overcoming increased DNA damage

Johanna Zerbib[1,13], Marica Rosaria Ippolito[2,13], Yonatan Eliezer[1], Giuseppina De Feudis[2], Eli Reuveni[1], Anouk Savir Kadmon[1], Sara Martin[2], Sonia Viganò[2], Gil Leor[1], James Berstler[3], Julia Muenzner[4], Michael Mülleder[5], Emma M. Campagnolo[6], Eldad D. Shulman[6], Tiangen Chang[6], Carmela Rubolino[7], Kathrin Laue[1], Yael Cohen-Sharir[1], Simone Scorzoni[2], Silvia Taglietti[2], Alice Ratti[2], Chani Stossel[8,9], Talia Golan[8,9], Francesco Nicassio[7], Eytan Ruppin[6], Markus Ralser[4,10,11], Francisca Vazquez[3], Uri Ben-David[1,14], Stefano Santaguida[2,12,14]

[1] Department of Human Molecular Genetics and Biochemistry, Faculty of Medicine, Tel Aviv University, Tel Aviv, Israel
[2] Department of Experimental Oncology at IEO, European Institute of Oncology IRCCS, Milan, Italy
[3] Broad Institute of MIT and Harvard, Cambridge, MA, USA
[4] Charité Universitätsmedizin Berlin, Department of Biochemistry, Berlin, Germany
[5] Charité Universitätsmedizin Berlin, Core Facility High-Throughput Mass Spectrometry, Berlin, Germany
[6] Cancer Data Science Laboratory, Center for Cancer Research, National Cancer Institute, National Institutes of Health, Bethesda, MD, USA
[7] Center for Genomic Science of IIT@SEMM, Fondazione Instituto Italiano di Technologia, Milan, Italy
[8] Oncology Institute, Sheba Medical Center, Tel Hashomer, Israel
[9] Faculty of Medicine, Tel Aviv University, Tel Aviv, Israel
[10] Nuffield Department of Medicine, University of Oxford, Oxford, United Kingdom
[11] Max Planck Institute for Molecular Genetics, Berlin, Germany
[12] Department of Oncology and Hemato-Oncology, University of Milan, Milan, Italy
[13] These authors contributed equally: Johanna Zerbib, Marica Ippolito
[14] These authors jointly supervised this work: Uri Ben-David, Stefano Santaguida

Correspondence: Uri Ben-David (ubendavid@tauex.tau.ac.il), Stefano Santaguida (Stefano.santaguida@ieo.it)

This file contains:

- 12 Supplementary Figures and their Legends
- 2 Supplementary Tables

Supplementary Figures

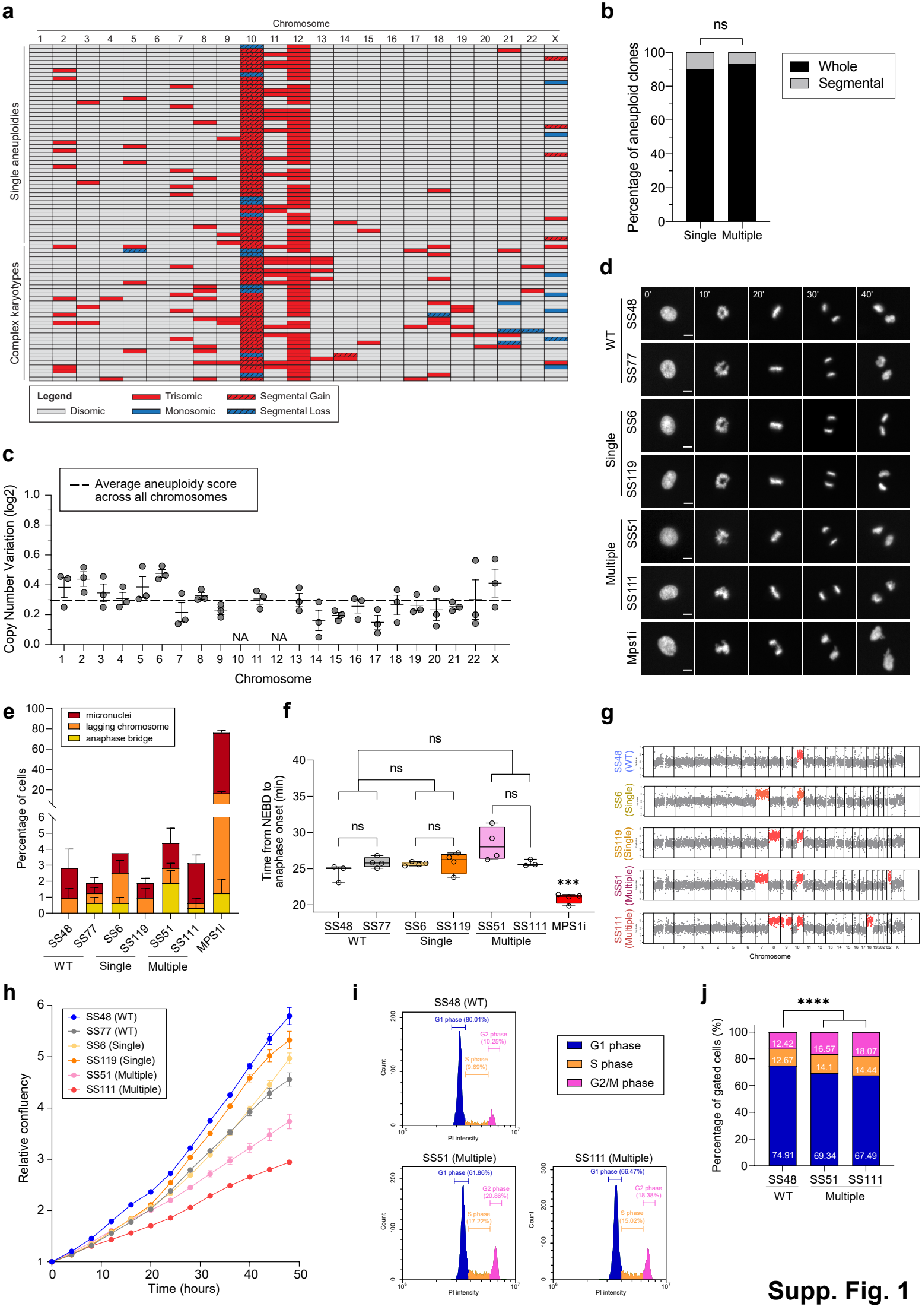
a
Chromosome
1 2 3 4 5 6 7 8 9 10 11 12 13 14 15 16 17 18 19 20 21 22 X
Single aneuploidies
Complex karyotypes
Legend
Disomic
Trisomic
Monosomic
Segmental Gain
Segmental Loss
b
ns
Percentage of aneuploid clones
Whole
Segmental
Single
Multiple
c
Average aneuploidy score across all chromosomes
Copy Number Variation (log2)
NA
NA
Chromosome
d
0'
10'
20'
30'
40'
WT
SS48
SS77
Single
SS6
SS119
Multiple
SS51
SS111
Mps1i
e
micronuclei
lagging chromosome
anaphase bridge
Percentage of cells
SS48
SS77
SS6
SS119
SS51
SS111
MPS1i
WT
Single
Multiple
f
ns
***
Time from NEBD to anaphase onset (min)
SS48
SS77
SS6
SS119
SS51
SS111
MPS1i
WT
Single
Multiple
g
SS48 (WT)
SS6 (Single)
SS119 (Single)
SS51 (Multiple)
SS111 (Multiple)
Chromosome
h
SS48 (WT)
SS77 (WT)
SS6 (Single)
SS119 (Single)
SS51 (Multiple)
SS111 (Multiple)
Relative confluency
Time (hours)
i
SS48 (WT)
G1 phase (80.01%)
G2 phase (10.25%)
S phase (9.69%)
SS51 (Multiple)
G1 phase (61.86%)
G2 phase (20.86%)
S phase (17.22%)
SS111 (Multiple)
G1 phase (66.47%)
G2 phase (18.38%)
S phase (15.02%)
Count
PI intensity
G1 phase
S phase
G2/M phase
j
****
Percentage of gated cells (%)
12.42
12.67
74.91
16.57
14.1
69.34
18.07
14.44
67.49
SS48
SS51
SS111
WT
Multiple

Supp. Fig. 1

Supplementary Figure 1: Characterization of the matched aneuploid and pseudo-diploid clones (related to Fig. 1)

(a) Karyotypes of the 79 RPE1 aneuploid clones, derived by transient reversine treatment of the parental RPE1 population. Each row represents one single cell-derived clone. **(b)** Percentage of aneuploid clones harboring whole (black) or segmental (gray) aneuploidies. Chromosomes 10 and 12 were excluded, as trisomy of chromosome 12 and gain of chromosome 10q are clonal events. There are no differences in segmental and whole chromosome aneuploidy composition ($p=0.61$, Fisher's exact test). **(c)** Aneuploidy scores (defined as log2(CNV) of each chromosome) of RPE1 cells immediately following aneuploidy induction using reversine. Dashed line indicates the average CNV across all chromosomes. Chromosomes 10 and 12 were excluded, as trisomy of chromosome 12 and gain of chromosome 10q are clonal events. n=3 independent experiments. NA: not applicable. No significant differences were found (Kruskal-Wallis test, Dunn's multiple comparisons), and no correlation was found between reversine pulse and the final library ($rho=0.18$, $p=0.42$; Spearman's correlation). (**d**) Representative live cell images of dividing cells in RPE1 clones.Reversine-treated parental RPE1is shown as positive control. Scale bar, 10μm (**e**) Detailed quantification of aberrant mitosis events (micronuclei, lagging chromosomes, anaphase bridges) in the RPE1 clones. Reversine was used as positive control. n=4 independent experiments. **(f)** Mitotic timing of pseudo-diploid (SS48, SS77 and SS31) and aneuploid (SS6, SS119, SS51, SS111) clones, determined by live-cell imaging and measured from nuclear envelope breakdown to anaphase onset. Reversine was used as positive control. n=3 (SS48, SS111) or n=4 (SS77, SS6, SS119, SS51, MPS1i) independent experiments. n.s., $p>0.05$; ***, $p<0.001$; One-way ANOVA, Tukey's multiple comparison test. **(g)** Low-pass whole-genome sequencing (lp-WGS) copy number profiles of pseudo-diploid (SS48 and SS77) and aneuploid (SS6, SS119, SS51, SS111) clones after 10 passages in culture. Chromosome gains are colored in red, including the clonal gain of the q-arm of chromosome 10. **(h)** Representative proliferation curves of aneuploid RPE1 clones. Relative confluency was estimated during 48hrs. n=5 independent experiments. (**i**) Representative cell cycle analyses of pseudo-diploid (SS48) and highly-aneuploid (SS51, SS111) clones. Cell cycle phases are color-coded. (**j**) Proportion of cells across cell cycle phases in pseudo-diploid (SS48) and highly-aneuploid (SS51, SS111) clones. The proportion of cells in the G2/M phase is significantly higher in the highly-aneuploid clones. ****, $p<0.0001$; Chi-square test. Source data are provided as a Source Data file.

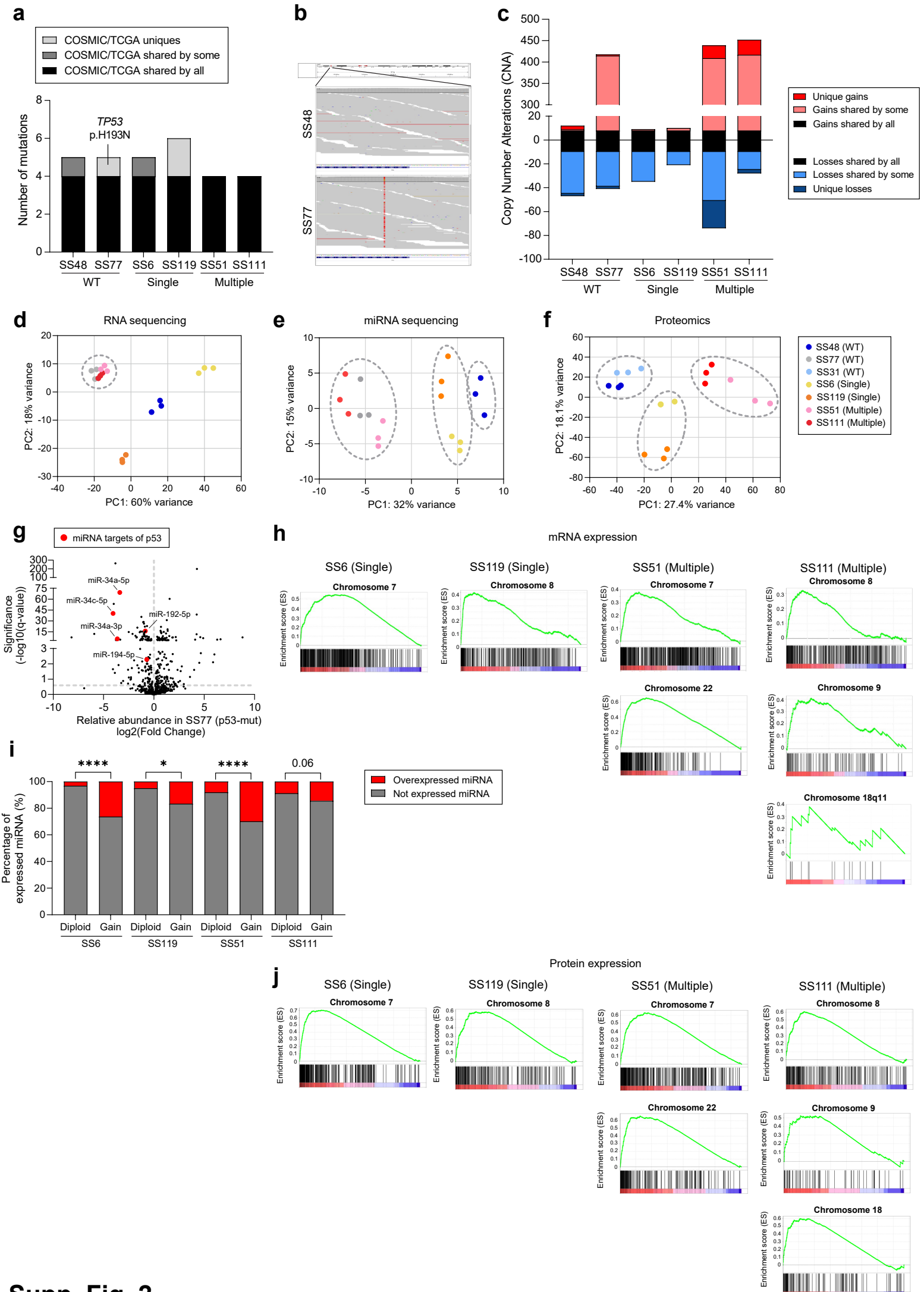
a
COSMIC/TCGA uniques
COSMIC/TCGA shared by some
COSMIC/TCGA shared by all
Number of mutations
TP53
p.H193N
SS48 SS77 SS6 SS119 SS51 SS111
WT
Single
Multiple
b
SS48
SS77
c
Copy Number Alterations (CNA)
Unique gains
Gains shared by some
Gains shared by all
Losses shared by all
Losses shared by some
Unique losses
SS48 SS77 SS6 SS119 SS51 SS111
WT
Single
Multiple
d
RNA sequencing
PC2: 18% variance
PC1: 60% variance
e
miRNA sequencing
PC2: 15% variance
PC1: 32% variance
f
Proteomics
PC2: 18.1% variance
PC1: 27.4% variance
SS48 (WT)
SS77 (WT)
SS31 (WT)
SS6 (Single)
SS119 (Single)
SS51 (Multiple)
SS111 (Multiple)
g
miRNA targets of p53
miR-34a-5p
miR-34c-5p
miR-34a-3p
miR-192-5p
miR-194-5p
Significance (-log10(q-value))
Relative abundance in SS77 (p53-mut)
log2(Fold Change)
h
mRNA expression
SS6 (Single)
SS119 (Single)
SS51 (Multiple)
SS111 (Multiple)
Chromosome 7
Chromosome 8
Chromosome 22
Chromosome 9
Chromosome 18q11
Enrichment score (ES)
i
****
*
****
0.06
Overexpressed miRNA
Not expressed miRNA
Percentage of expressed miRNA (%)
Diploid Gain Diploid Gain Diploid Gain Diploid Gain
SS6 SS119 SS51 SS111
j
Protein expression
SS6 (Single)
SS119 (Single)
SS51 (Multiple)
SS111 (Multiple)
Chromosome 7
Chromosome 8
Chromosome 22
Chromosome 9
Chromosome 18
Enrichment score (ES)

Supp. Fig. 2

Supplementary Figure 2: Systematic genomic characterization of RPE1 clones (related to Fig. 2)

(a) Mutation profiles across the RPE1 clones obtained from the Whole Exome Sequencing. SS77 acquired a heterozygous *TP53*-inactivating mutation (p.H193N), turning it into a p53-mutated clone. **(b)** IGV-based visualization of the *TP53* locus of SS48 and SS77, demonstrating the acquisition of a clonal (AF~0.5) heterozygous p53-inactivating mutation (p.H193N) in SS77 clone. **(c)** Copy number alterations (CNAs) across the RPE1 clones, including SS77. SS77 shares an elevated number of CNAs with the highly-aneuploid clones. **(d-f)** Principal Component Analysis (PCA) of the genome-wide mRNA **(d)**, miRNA (**e**) and proteomics (**f**) expression profiles of the RPE1 clones. PC1 and PC2 explain 60% and 18% (**d**), 32% and 15% (**e**), and 27.4% and 18.1% (**f**) of the variance between the samples, respectively. Notably, SS51, SS111 and SS77 cluster together. **(g)** Relative miRNA abundance between SS48 and SS77, showing downregulation of p53-targeting miRNAs in SS77. Significance threshold set at qvalue=0.25. p53-targeting miRNAs are highlighted in red. **(h)** GSEA plots of the mRNA dataset, demonstrating the chromosomal-level positional enrichment to the specific gained chromosome(s) in each RPE1 clone. Comparison between the control clone (SS48) and the various aneuploid clones (SS6, SS119, SS51, SS111). Enrichments scores : SS6 (NES=2.00, qvalue<0.0001), SS119 (NES=2.5, qvalue<0.0001), SS51 (chr7 : NES=2.42, qvalue<0.0001 ; chr22 : NES=3.88, qvalue<0.0001), SS111 (chr8 : NES=1.92, qvalue=0.0065 ; chr9 : NES=2.04, qvalue=0.0055 ; chr18Q11 : NES=1.22, qvalue=0.1988). (**i**) Comparison of the over-expressed miRNAs between the gained and the diploid chromosome(s) in RPE1 clones (SS6: chr7; SS119: chr8; SS51: chr7, chr22; SS111: chr8, chr9, chr18). p=0.06 for SS111, *, p=0.03 and ****, p<0.0001 for SS119, SS6 and SS51, respectively; Chi-square test. **(j)** GSEA plots of the proteomics dataset, demonstrating the chromosomal-level positional enrichment to the specific gained chromosome(s) in each RPE1 clone. Comparison between the control clone (SS48) and the various aneuploid clones (SS6, SS119, SS51, SS111). Enrichments scores : SS6 (NES=2.65, qvalue<0.0001), SS119 (NES=2.02, qvalue<0.0001), SS51 (chr7 : NES=2.12, qvalue<0.0001 ; chr22 : NES=2.15, qvalue<0.0001), SS111 (chr8 : NES=2.21, qvalue=0.0065 ; chr9 : NES=1.61, qvalue=0.0011 ; chr18: NES=2.02, qvalue<0.0001). Source data are provided as a Source Data file.

a

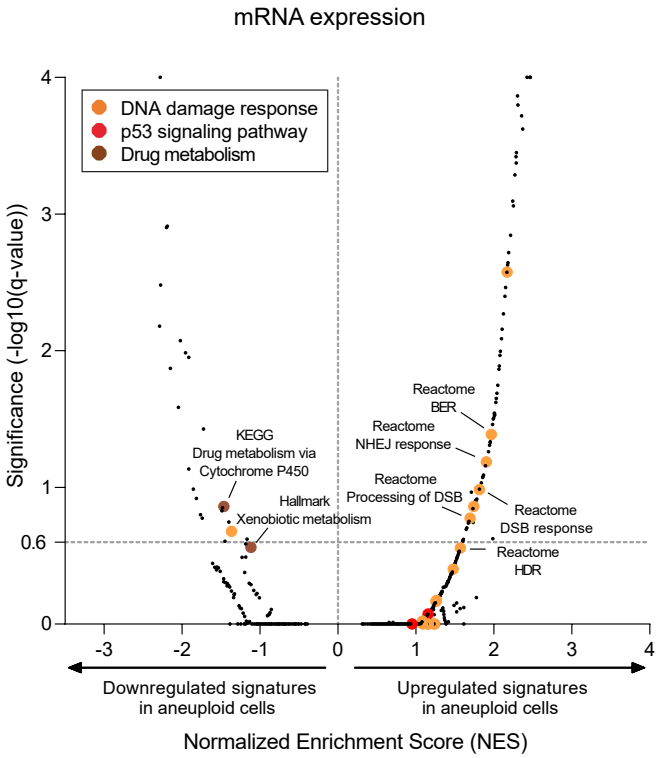

b

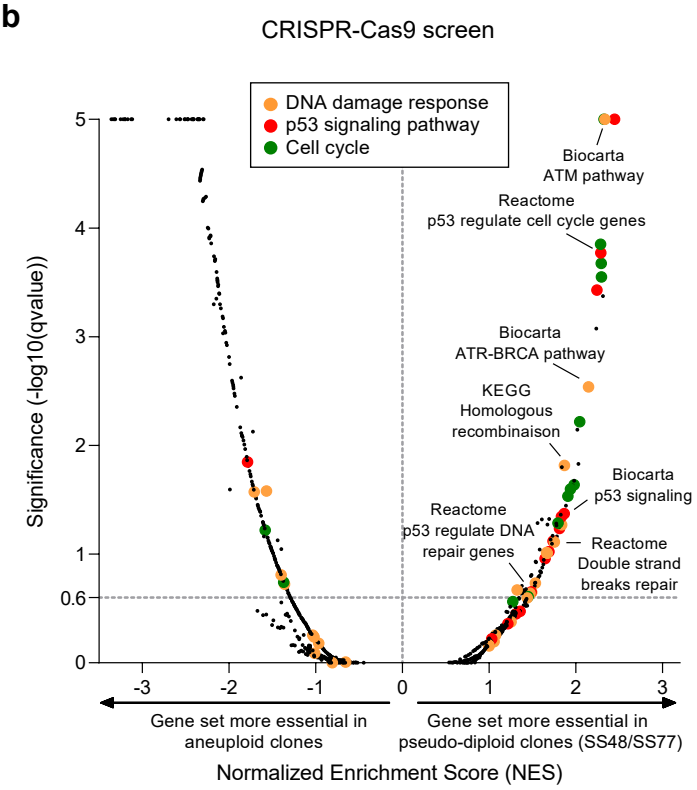

c

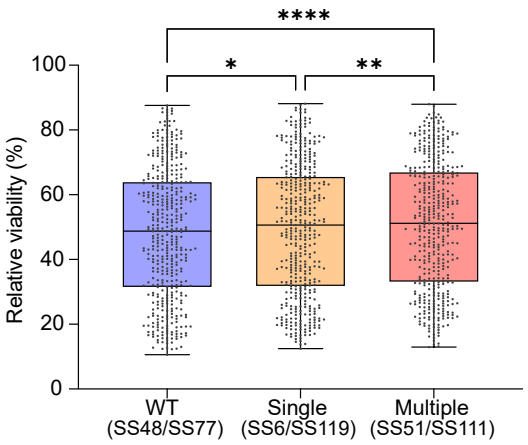

Supp. Fig. 3

Supplementary Figure 3: Systematic functional characterization of RPE1 clones (related to Fig. 2)

(a) Comparison of the differential gene expression patterns (pre-ranked GSEA results) between the near-diploid SS48 clone (control) and the aneuploid SS6, SS119, SS51 and S111 clones. Plot presents enrichments for the Hallmark, KEGG, Biocarta and Reactome gene sets. Significance threshold set at qvalue=0.25. Enriched pathways are color-coded. **(b)** Comparison of the differential gene dependency scores (pre-ranked GSEA results) between the near-diploid SS48 and SS77 clones (control) and the aneuploid SS6, SS119 and SS51 clones. Plot presents enrichments for the Hallmark, KEGG, Biocarta and Reactome gene sets. Significance threshold set at qvalue=0.25. Enriched pathways are color-coded. **(c)** Comparison of overall drug sensitivity between the near-diploid control clone (SS48 and SS77), clones with a single trisomy (SS6 and SS119), and clones with multiple trisomies (SS51 and SS111). Only drugs that led to a viability reduction ranging from -10% to -90% compared to DMSO control (see Methods) were considered (n=439 drugs). *, p=0.0119 (Single/WT), ****p<0.0001 (Multiple/WT), **, p=0.0032 (Single/Multiple); Repeated-Measures One-Way ANOVA, Tukey's multiple comparison. Source data are provided as a Source Data file.

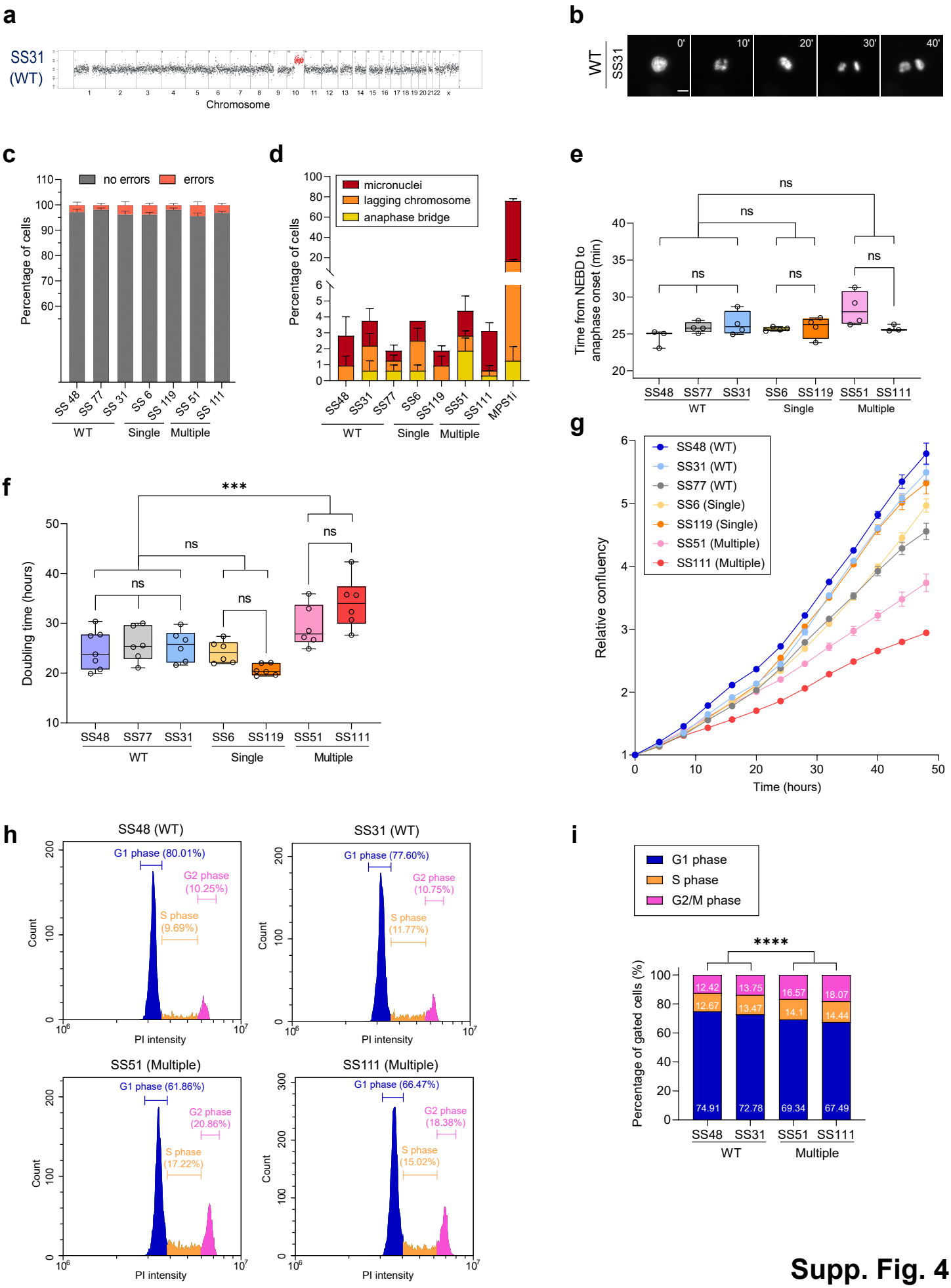
a
SS31 (WT)
Chromosome
b
WT
SS31
0'
10'
20'
30'
40'
c
no errors
errors
Percentage of cells
SS 48
SS 77
SS 31
SS 6
SS 119
SS 51
SS 111
WT
Single
Multiple
d
micronuclei
lagging chromosome
anaphase bridge
Percentage of cells
SS48
SS31
SS77
SS6
SS119
SS51
SS111
MPS1i
WT
Single
Multiple
e
Time from NEBD to anaphase onset (min)
ns
SS48
SS77
SS31
SS6
SS119
SS51
SS111
WT
Single
Multiple
f
Doubling time (hours)
***
ns
SS48
SS77
SS31
SS6
SS119
SS51
SS111
WT
Single
Multiple
g
Relative confluency
Time (hours)
SS48 (WT)
SS31 (WT)
SS77 (WT)
SS6 (Single)
SS119 (Single)
SS51 (Multiple)
SS111 (Multiple)
h
SS48 (WT)
G1 phase (80.01%)
G2 phase (10.25%)
S phase (9.69%)
SS31 (WT)
G1 phase (77.60%)
G2 phase (10.75%)
S phase (11.77%)
SS51 (Multiple)
G1 phase (61.86%)
G2 phase (20.86%)
S phase (17.22%)
SS111 (Multiple)
G1 phase (66.47%)
G2 phase (18.38%)
S phase (15.02%)
Count
PI intensity
i
G1 phase
S phase
G2/M phase
****
Percentage of gated cells (%)
12.42
12.67
74.91
13.75
13.47
72.78
16.57
14.1
69.34
18.07
14.44
67.49
SS48
SS31
SS51
SS111
WT
Multiple

Supp. Fig. 4

Supplementary Figure 4: Characterization of pseudo-diploid clone SS31 (related to Fig.1 and Fig.2)

(a) Low-pass whole-genome sequencing (lp-WGS) copy number profile, showing the karyotype of the pseudo-diploid SS31 clone, derived from RPE1 cells. Chromosome gains are colored in red, including the clonal gain of the q-arm of chromosome 10. (**b**) Representative live cell images of the mitotic phases in the SS31 clone. Scale bar, 10μm. **(c)** Quantification of chromosome segregation errors as in Figure 1E. The graph shows the same value shown in Figure 1E, with the addition of clone SS31. Graph shows the average of four biological replicates ± SEM. (**d**) Detailed quantification of aberrant mitosis events (micronuclei, lagging chromosomes, anaphase bridges), as in Supplementary Fig. 1e. The graph shows the same data shown in Supplementary Fig. 1e, with the addition of the pseudo-diploid clone SS31. **(e)** Quantification of mitotic timing of pseudo-diploid (SS48, SS77 and SS31) and aneuploid (SS6, SS119, SS51, SS111) clones. Mitotic timings were determined by live-cell imaging of clones that stably express green fluorescent protein fused to histone H2B (H2B-GFP). Mitotic timing was measured from nuclear envelope breakdown to anaphase onset. Treatment with reversine, the MPS1 inhibitor, was used as positive control. The graph shows the same data shown in Supplementary Fig. 1f, with the addition of clone SS31. n.s., $p>0.05$; One-way ANOVA, followed by Tukey's multiple comparison test. **(f)** Doubling time quantification as in Figure 1F, including SS31. N=7 (SS48) and n=6 (SS77, SS31, SS6, SS119, SS51, SS111) independent experiments. n.s., $p>0.25$; * $p=0.032$; **, $p=0.003$; One-way ANOVA, Tukey's multiple comparison. **(g)** Representative proliferation curves of SS48, SS77, SS31, SS6, SS119, SS51 and SS111. Relative confluency was estimated every 4hrs during 48hrs. The proliferation curves show the same data as in Figure S1F, with the addition of clone SS31. (**h**) Representative flow cytometry cell cycle analyses, as presented in Supplementary Fig. 1i, with the addition of clone SS31. (**i**) Comparison of the proportion of cells across cell cycle phases in pseudo-diploid (SS48) and highly-aneuploid (SS51, SS111) clones, as presented in Supplementary Fig. 1j, with the addition of clone SS31. ****, $p<0.0001$; Chi-square test. Source data are provided as a Source Data file.

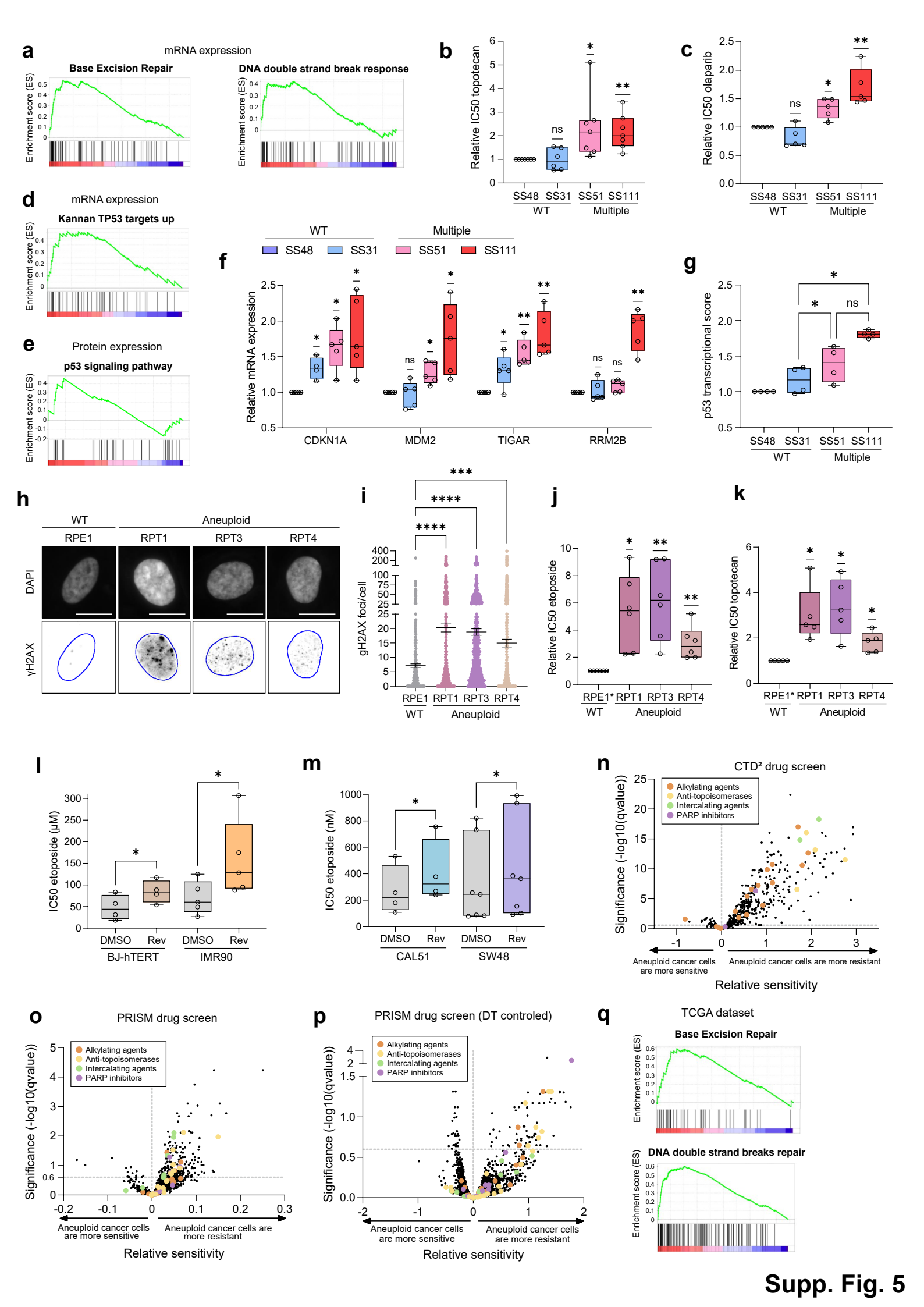
a
mRNA expression
Base Excision Repair
DNA double strand break response
Enrichment score (ES)
b
Relative IC50 topotecan
c
Relative IC50 olaparib
SS48 SS31 SS51 SS111
WT
Multiple
d
mRNA expression
Kannan TP53 targets up
e
Protein expression
p53 signaling pathway
f
WT
Multiple
SS48 SS31 SS51 SS111
Relative mRNA expression
CDKN1A
MDM2
TIGAR
RRM2B
g
p53 transcriptional score
h
WT
Aneuploid
RPE1 RPT1 RPT3 RPT4
DAPI
γH2AX
i
gH2AX foci/cell
RPE1 RPT1 RPT3 RPT4
WT
Aneuploid
j
Relative IC50 etoposide
k
Relative IC50 topotecan
l
IC50 etoposide (μM)
DMSO Rev DMSO Rev
BJ-hTERT
IMR90
m
IC50 etoposide (nM)
CAL51
SW48
n
CTD² drug screen
Alkylating agents
Anti-topoisomerases
Intercalating agents
PARP inhibitors
Significance (-log10(qvalue))
Aneuploid cancer cells are more sensitive
Aneuploid cancer cells are more resistant
Relative sensitivity
o
PRISM drug screen
p
PRISM drug screen (DT controled)
q
TCGA dataset
Base Excision Repair
DNA double strand breaks repair

Supp. Fig. 5

Supplementary Figure 5: Increased DDR in response to aneuploidy (related to Fig. 3)

(a) GSEA of DDR, comparing the highly-aneuploid clones, SS51 and SS111, to the pseudo-diploid clone SS48. Shown are enrichment plots for the Reactome 'Base Excision Repair' (NES=2.75, q-value<0.001) and 'Double Strand Break Response' (NES=2.05, q-value=0.0026) gene sets. **(b)** Drug sensitivity to 72hr drug treatment with topotecan, between pseudo-diploid and highly-aneuploid clones . n=6 (SS31) and n=7 (SS48, SS51, SS111) independent experiments. IC50 fold-change calculated relative to SS48, per experiment. *, p=0.039 and **, p=0.0062 for SS51 and SS111 respectively; two-tailed One-Sample t-test. (**c**) Drug sensitivity to 72hr drug treatment with olaparib, between pseudo-diploid clones and highly-aneuploid clones . n=5 independent experiments. IC50 fold-change calculated relative to SS48, per experiment. *, p=0.0135 and **, p=0.0098 for SS51 and SS111 respectively; One-Sample t-test. **(d)** GSEA of p53-related gene expression signatures in the transcriptomic dataset, comparing the highly-aneuploid clones, SS51 and SS11, to the pseudo-diploid clone SS48 ('Kannan_TP53_Targets_Up' gene set; NES=2.09, q-value=0.004). **(e)** GSEA of p53-related signatures in the proteomic dataset, comparing highly-aneuploid clones SS51 and SS111, to the pseudo-diploid clones SS48 and SS31('KEGG p53 signaling pathway' gene set; NES=1.38, p-value=0.053). **(f)** Comparison of the mRNA expression levels of the p53 transcriptional targets, between pseudo-diploid clones and highly-aneuploid clones . n=5 independent experiments. CDKN1A (p21): *, p=0.0207, p=0.0104 and p=0.0282 for SS31, SS51 and SS111, respectively; MDM2: *, p=0.0175 and p=0.0315 for SS51 and SS111 respectively; TIGAR: *, p=0.0386 and **, p=0.0028 and p=0.0049 for SS31, SS51 and SS111 respectively; RRM2B: **, p=0.0024 (SS111); One-Sample t-test. **(g)** p53 transcriptional score (p53 activation pathway) in each RPE1 clone. Each dot represents the averaged gene expression of each target, as presented in Supplementary Fig. 5f (GADD45A is excluded). p53 activation is stronger in highly-aneuploid clones compared to pseudo-diploid clone SS31. n=4 targets, *, p=0.05 and p=0.0134 for SS31/SS51 and SS31/SS111 respectively; One-Way RM ANOVA. **(h)** IF of γH2AX foci in pseudo-diploid RPE1 cells, and their highly-aneuploid derivatives RPTs. Scale bar, 5µm. **(i)** Quantification of γH2AX foci between pseudo-diploid RPE1* and highly aneuploid RPT cells. n=6 independent experiments, ~100 nuclei analyzed per experiment; ***, p=0.0004 (RPT4/RPE1) and ****, p<0.0001 (RPT1/RPE1, RPT3/RPE1); Kruskal-Wallis test, Dunn's multiple comparison. **(j)** Drug sensitivity to 72hr treatment with etoposide, between pseudo-diploid RPE1 cells, and their highly-aneuploid derivatives RPTs. n=6 independent experiments. IC50 fold-change was calculated relative to RPE1, per experiment. *, p=0.0126, **, p=0.0072 and p=0.0095 for RPT1, RPT3 and RPT4, respectively; two-tailed One-Sample t-test. **(k)** Drug sensitivity to 72hr treatment with topotecan, between pseudo-diploid RPE1 cells, and their highly-aneuploid derivatives RPTs. n=5 independent experiments. IC50 fold-change was calculated relative to RPE1, per experiment. *, p=0.0208, p=0.0145, p=0.016 for RPT1, RPT3 and RPT4 respectively; two-tailed One-Sample t-test. (**l-m**) Sensitivity of additional non-transformed (**l**, BJ-hTERT and IMR90) and cancer (**m**, CAL51 and SW48) cell lines to etoposide, following aneuploidy induction using reversine (see Methods). (**l**) n=4 independent experiments, per cell line; *, p=0.048 and p=0.030 for BJ-hTERT and IMR90, respectively; two-sided paired t-test. (**m**) n=4 (CAL51) and n=7 (SW48) independent experiments; *, p=0.027 and p=0.019, for CAL51 and SW48, respectively; two-sided paired t-test. **(n-p)** Differential drug sensitivities between near-euploid and highly-aneuploid human cancer cell lines, based on the large-scale CTD^2 drug screen[46] (**n**), PRISM screen[48] (**o**), and doubling-time controlled PRISM screen. (**p**). Data are taken from Cohen-Sharir *et al*[7]. (**n-o**) and PRISM screen 23Q2 released (**p**), doubling time of the cancer cell lines from Tscherniak *et al*[45]. Direct DNA damage inducers are highlighted in orange, green, yellow and purple, respectively. Highly-aneuploid cell lines are more resistant to these drugs, independently of their proliferation index (p=0.007, Chi-square test). (**q**) Pre-ranked GSEA of mRNA expression levels showing that high aneuploidy levels are associated with upregulation of the DNA damage response (DDR) in human primary tumors. Shown is the enrichment plot of Reactome 'Base excision repair' (NES=2.00; q-value=0.001) and 'DNA double strand repair' (NES=2.43, qvalue<0.001) gene sets. Data were obtained from the TCGA mRNA expression dataset[99]. Source data are provided as a Source Data file.

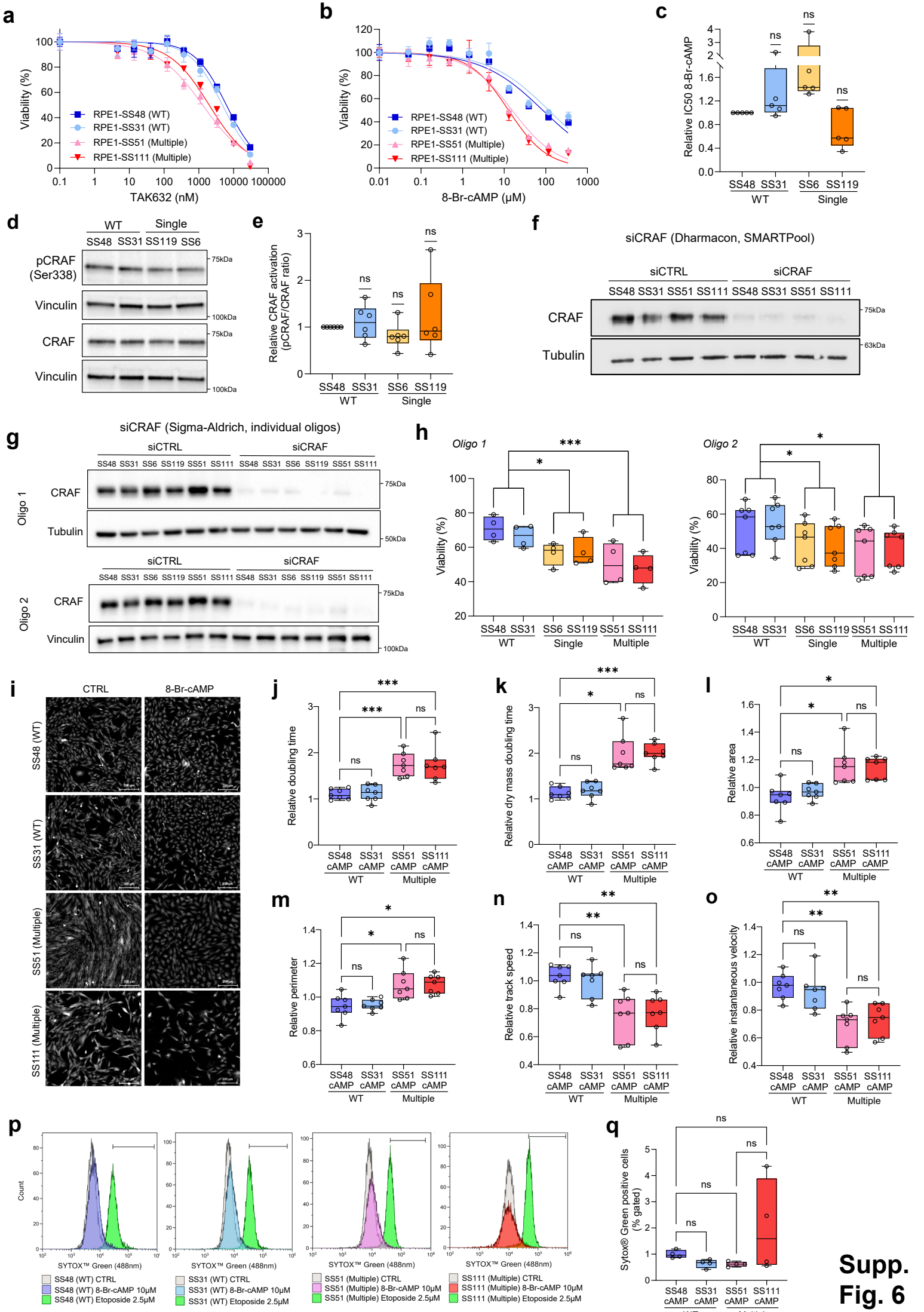
a
Viability (%)
TAK632 (nM)
RPE1-SS48 (WT)
RPE1-SS31 (WT)
RPE1-SS51 (Multiple)
RPE1-SS111 (Multiple)
b
Viability (%)
8-Br-cAMP (μM)
c
Relative IC50 8-Br-cAMP
ns
SS48 SS31 SS6 SS119
WT Single
d
WT Single
SS48 SS31 SS119 SS6
pCRAF (Ser338)
Vinculin
CRAF
Vinculin
75kDa
100kDa
e
Relative CRAF activation (pCRAF/CRAF ratio)
f
siCRAF (Dharmacon, SMARTPool)
siCTRL siCRAF
SS48 SS31 SS51 SS111 SS48 SS31 SS51 SS111
CRAF
Tubulin
75kDa
63kDa
g
siCRAF (Sigma-Aldrich, individual oligos)
siCTRL siCRAF
SS48 SS31 SS6 SS119 SS51 SS111 SS48 SS31 SS6 SS119 SS51 SS111
Oligo 1
Oligo 2
CRAF
Tubulin
Vinculin
75kDa
50kDa
100kDa
h
Oligo 1
Oligo 2
Viability (%)
SS48 SS31 SS6 SS119 SS51 SS111
WT Single Multiple
i
CTRL
8-Br-cAMP
SS48 (WT)
SS31 (WT)
SS51 (Multiple)
SS111 (Multiple)
j
Relative doubling time
k
Relative dry mass doubling time
l
Relative area
m
Relative perimeter
n
Relative track speed
o
Relative instantaneous velocity
SS48 cAMP SS31 cAMP SS51 cAMP SS111 cAMP
WT Multiple
p
Count
SYTOX™ Green (488nm)
SS48 (WT) CTRL
SS48 (WT) 8-Br-cAMP 10μM
SS48 (WT) Etoposide 2.5μM
SS31 (WT) CTRL
SS31 (WT) 8-Br-cAMP 10μM
SS31 (WT) Etoposide 2.5μM
SS51 (Multiple) CTRL
SS51 (Multiple) 8-Br-cAMP 10μM
SS51 (Multiple) Etoposide 2.5μM
SS111 (Multiple) CTRL
SS111 (Multiple) 8-Br-cAMP 10μM
SS111 (Multiple) Etoposide 2.5μM
q
Sytox® Green positive cells (% gated)
Supp. Fig. 6

Supplementary Figure 6: Characterization of CRAF activity and dependency in pseudo-diploid vs. highly-aneuploid RPE1 clones (related to Fig. 4)

(a-b) Representative curves of the drug response to TAK632 (**a**) and 8-Br-cAMP (**b**). Highly-aneuploid clones are colored in pink (SS51) and red (SS111), pseudo-diploid controls are colored in blue (SS48) and light blue (SS31). **(c)** Drug sensitivity to 72hr drug treatment with 8-Br-cAMP, between pseudo-diploid clones (SS48 and SS31) and single aneuploid clones (SS6 and SS119). IC50 fold-change relative to SS48, per experiment; two-tailed One-Sample t-test. **(d)** Western blot of pCRAF (Ser338) and total CRAF protein levels in pseudo-diploid clones (SS48 and SS31) and single trisomy clones (SS6 and SS119).**(e)** CRAF activation (pCRAF/CRAF ratio) calculated relative to SS48 per experiment. n=6 independent experiments; One-Sample t-test. **(f-g)** Western blot of total CRAF protein levels in siCRAF-treated RPE1 clones (or associated scrambled siRNA), using pooled siRNA ('SMARTPool' Dharmacon, (**f**) or individual oligos (Sigma-Aldrich, (**g**)) for 72hrs. **(h)** Viability following siCRAF in RPE1 clones, 72hrs post transfection. Viability calculated versus the scrambled siRNA, per experiment and per oligo. n=4 (oligo 1) and n=7 (oligo 2) independent experiments; oligo 1: *, p=0.014 (WT/Single), ***, p=0.0001 (WT/Multiple); oligo 2: *, p=0.048 (WT/Single) and p=0.017 (WT/Multiple); RM One-Way ANOVA, multiple comparison. **(i-o)** Live-cell imaging quantification of multiple cell parameters following CRAF inhibition using 10μM 8-Br-cAMP for 72h. Presented representative images (**i**) of cells treated with the drug. Comparison of doubling time (**j**), dry mass doubling time (**k**), cell area (**l**), cell perimeter (**m**), cell track speed (**n**) and cell velocity (**o**), between the pseudo-diploid and highly-aneuploid clones. n=7 independent experiments. Fold-change calculated relative to DMSO-treated cells; One-Way ANOVA, Tukey's multiple comparison. * $p<0.05$; ** $p<0.01$; *** $p<0.001$. **(p-q)** Cell death analysis following exposure to 10μM 8-Br-cAMP for 72hrs, using SYTOX™ Green. Etoposide (2.5μM for 72hr) was used as positive control (**p**). ~1% of 8-Br-cAMP-treated cells were SYTOX™-positive in both pseudo-diploid and highly aneuploid cells (**q**). n=4 independent experiments; n.s., $p>0.05$; One-way ANOVA with Tukey's multiple comparison. Source data are provided as a Source Data file.

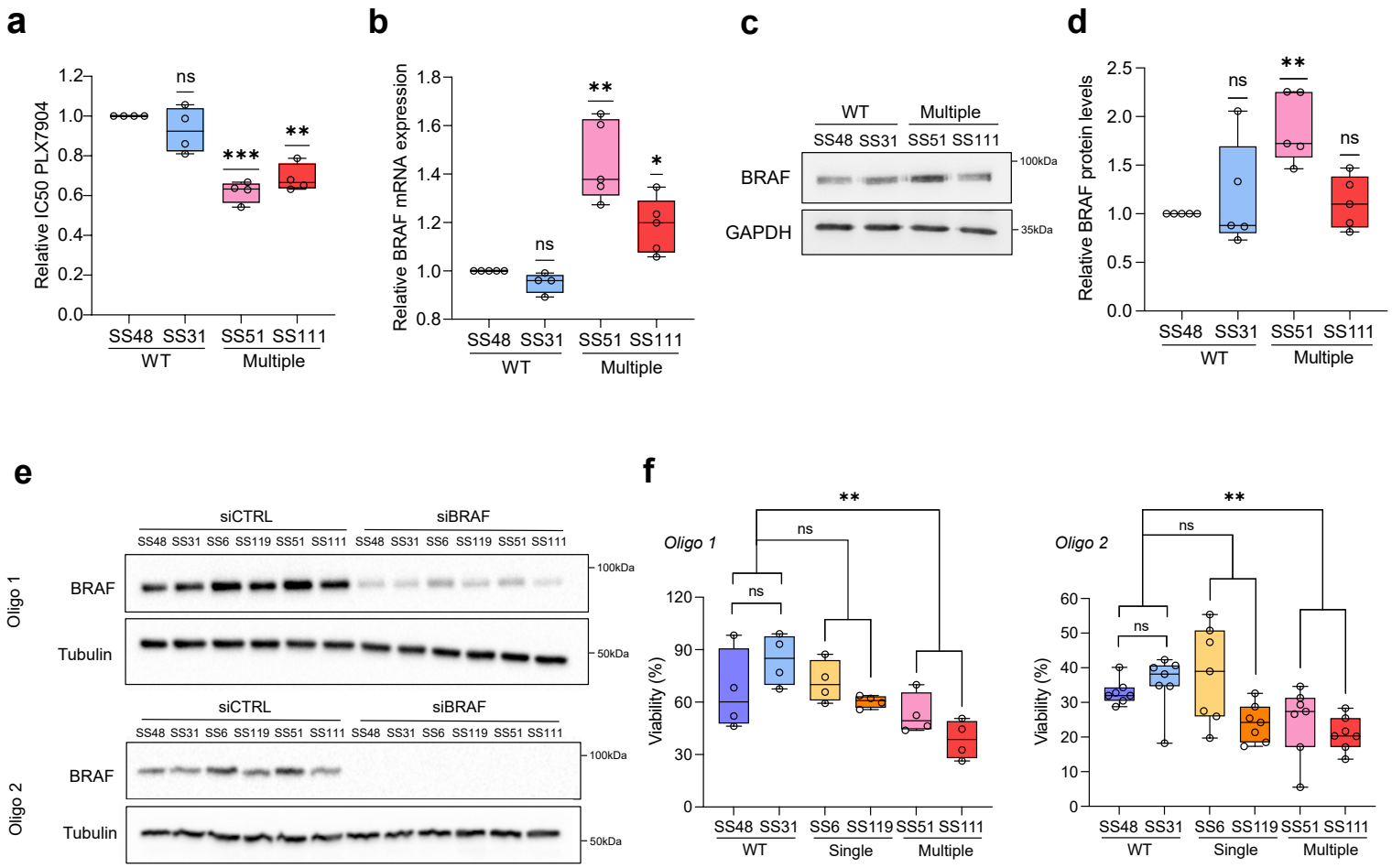
a
Relative IC50 PLX7904
ns
***
**
SS48 SS31 SS51 SS111
WT Multiple
b
Relative BRAF mRNA expression
**
ns
*
SS48 SS31 SS51 SS111
WT Multiple
c
WT Multiple
SS48 SS31 SS51 SS111
BRAF
GAPDH
100kDa
35kDa
d
Relative BRAF protein levels
ns
**
ns
SS48 SS31 SS51 SS111
WT Multiple
e
siCTRL siBRAF
SS48 SS31 SS6 SS119 SS51 SS111 SS48 SS31 SS6 SS119 SS51 SS111
Oligo 1
BRAF
Tubulin
100kDa
50kDa
Oligo 2
f
Oligo 1
Oligo 2
Viability (%)
**
ns
SS48 SS31 SS6 SS119 SS51 SS111
WT Single Multiple

Supp. Fig. 7

Supplementary Figure 7: Characterization of BRAF expression and dependency in pseudo-diploid vs. highly-aneuploid RPE1 clones (related to Fig. 4)

(a) Drug sensitivity to 72hr drug treatment with the CRAF/BRAF heterodimerization inhibitor PLX7904, between pseudo-diploid clones (SS48 and SS31) and highly-aneuploid clones (SS51 and SS111). n=4 independent experiments. IC50 fold-change calculated relative to SS48, per experiment. ***, p=0.0008, **, p=0.0029, for SS51 and SS111, respectively; One-Sample t-test. **(b)** Comparison of the mRNA expression levels of BRAF, quantified by qRT-PCR, between pseudo-diploid clones (SS48 and SS31) and highly-aneuploid clones (SS51 and SS111). n=5 independent experiments. Expression fold-change was calculated relative to SS48, per experiment. **, p=0.0037, *, p=0.022 for SS51 and SS111, respectively; One-Sample t-test. **(c)** Western blot of BRAF protein levels in RPE1 clones. GAPDH was used as housekeeping control. **(d)** Quantification of BRAF protein levels between pseudo-diploid clones (SS48 and SS31) and highly-aneuploid clones (SS51 and SS111). n=5 independent experiments. **, p=0.0054 for SS51; One Sample t-test. **(e)** Western blot of total BRAF protein levels in RPE1 clones treated with individual siRNAs against BRAF (or associated scrambled siRNA, Sigma-Aldrich) for 72hrs. Tubulin was used as a housekeeping control. **(f)** Comparison of viability following siRNA against BRAF in RPE1 clones, 72hrs post transfection. Viability was calculated versus the scrambled siRNA treated cells, per experiment and per oligo. n=4 (oligo 1) and n=7 (oligo 2) independent experiments; there are no differences between both pseudo-diploid controls treated with siBRAF (p=0.3743 and p=0.337 for oligo 1 and oligo 2 respectively, paired t-test); **, p=0.0017 (WT/Multiple, oligo 1) and p=0.0039 (WT/Multiple, oligo 2), RM One-Way ANOVA, multiple comparison. Source data are provided as a Source Data file.

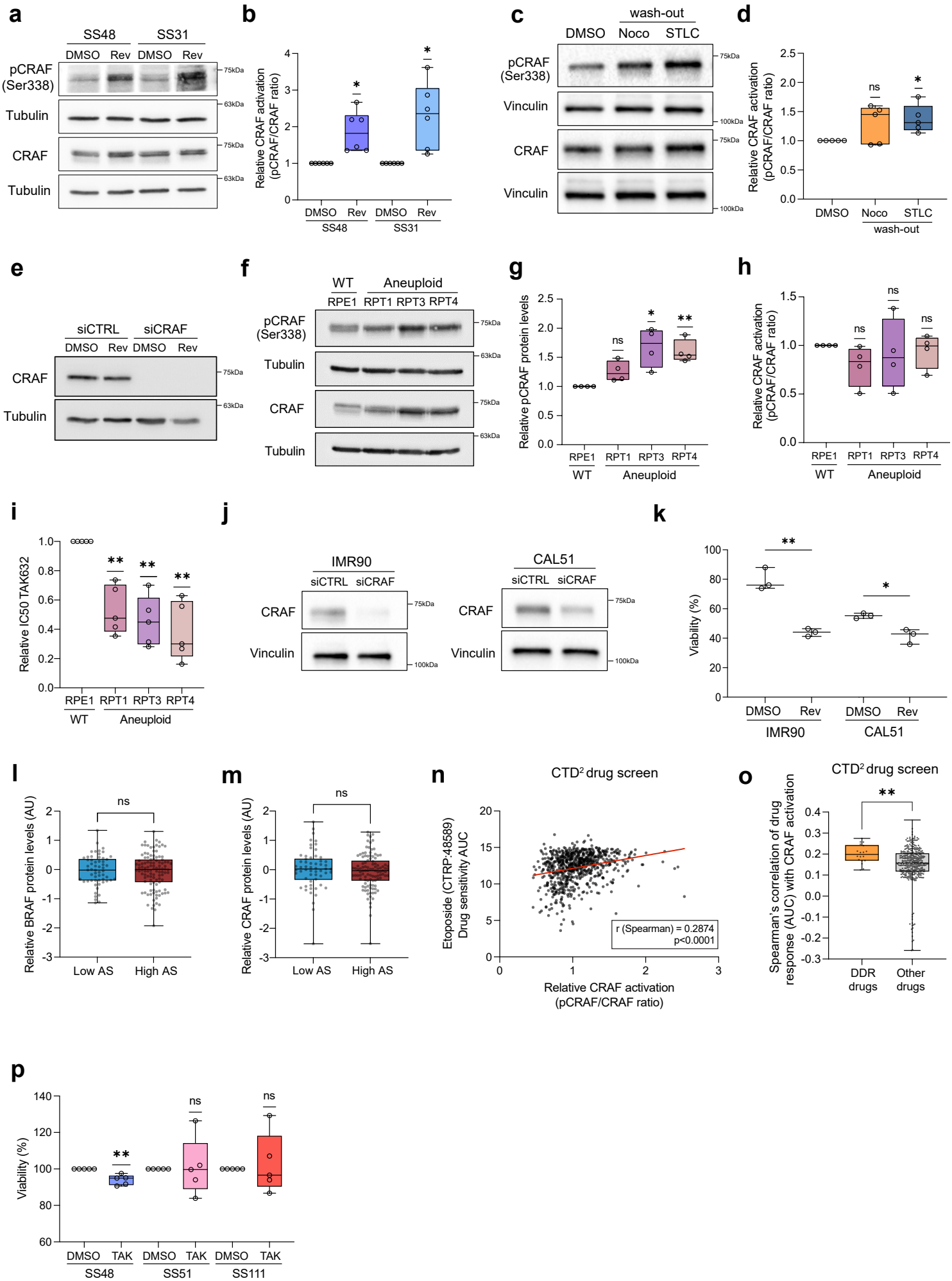
a
SS48
SS31
DMSO Rev DMSO Rev
pCRAF (Ser338)
Tubulin
CRAF
Tubulin
75kDa
63kDa
75kDa
63kDa
b
Relative CRAF activation (pCRAF/CRAF ratio)
DMSO Rev DMSO Rev
SS48 SS31
c
wash-out
DMSO Noco STLC
pCRAF (Ser338)
Vinculin
CRAF
Vinculin
75kDa
100kDa
75kDa
100kDa
d
Relative CRAF activation (pCRAF/CRAF ratio)
ns
DMSO Noco STLC
wash-out
e
siCTRL siCRAF
DMSO Rev DMSO Rev
CRAF
Tubulin
75kDa
63kDa
f
WT Aneuploid
RPE1 RPT1 RPT3 RPT4
pCRAF (Ser338)
Tubulin
CRAF
Tubulin
75kDa
63kDa
75kDa
63kDa
g
Relative pCRAF protein levels
ns
RPE1 RPT1 RPT3 RPT4
WT Aneuploid
h
Relative CRAF activation (pCRAF/CRAF ratio)
ns
ns
ns
RPE1 RPT1 RPT3 RPT4
WT Aneuploid
i
Relative IC50 TAK632
RPE1 RPT1 RPT3 RPT4
WT Aneuploid
j
IMR90
siCTRL siCRAF
CRAF
Vinculin
75kDa
100kDa
CAL51
siCTRL siCRAF
CRAF
Vinculin
75kDa
100kDa
k
Viability (%)
DMSO Rev DMSO Rev
IMR90 CAL51
l
Relative BRAF protein levels (AU)
ns
Low AS High AS
m
Relative CRAF protein levels (AU)
ns
Low AS High AS
n
CTD² drug screen
Etoposide (CTRP:48589) Drug sensitivity AUC
r (Spearman) = 0.2874
p<0.0001
Relative CRAF activation (pCRAF/CRAF ratio)
o
CTD² drug screen
Spearman's correlation of drug response (AUC) with CRAF activation
DDR drugs
Other drugs
p
Viability (%)
ns
ns
DMSO TAK DMSO TAK DMSO TAK
SS48 SS51 SS111

Supp. Fig. 8

Supplementary Figure 8: Validation of increased CRAF activity and dependency across various model systems (related to Fig. 4)

(a) Western blot of pCRAF and total CRAF protein levels in reversine-pulsed pseudo-diploid clones (SS48 and SS31) **(b)** CRAF activation (pCRAF/CRAF ratio) in reversine-pulsed pseudo-diploid clones relative to the DMSO control, per experiment. n=6 independent experiments. *, p=0.0124 and p=0.0162 for reversine-treated SS48 and SS31 cells, respectively; One Sample t-test. **(c)** Western blot of pCRAF and total CRAF protein levels in aneuploidy-induced parental RPE1 cells using nocodazole or STLC **(d)** CRAF activation (pCRAF/CRAF ratio) in aneuploidy-inducedRPE1 cells, calculated relative to the DMSO control per experiment. n=5 independent experiments. *, p=0.0254 (STLC-treated cells); One Sample t-test. **(e)** Western blot of CRAF protein levels in reversine-treated parental RPE1 cells, treated with siCRAF (or control siRNA, 'SMARTPool' Dharmacon) for 72hrs. **(f)** Western blot of phospho-CRAF and total CRAF protein levels in RPE/RPT cells. **(g-h)** Quantification of pCRAF protein levels (**g**) and CRAF activation (pCRAF/CRAF ratio, (**h**)) in RPE/RPT cells. n=4 independent experiments. pCRAF levels: p=0.059, *, p=0.0281, **, p=0.0087, for RPT1, RPT3, and RPT4 respectively; One Sample t-test. **(i)** Drug sensitivity to 72hr treatment with TAK632 in RPE/RPTs cells. n=5 independent experiments. IC50 fold-change was calculated relative to RPE1 per experiment. **, p=0.0032, p=0.002, p=0.0023, for RPT1, RPT3, and RPT4 respectively; One-Sample t-test. **(j)** Western blot of CRAF protein levels in reversine-treated non-transformed IMR90 (left) and cancer CAL51 (right) cell lines, treated with siCRAF (or control siRNA, 'SMARTPool' Dharmacon) for 72hrs. **(k)** Viability following siCRAF in aneuploidy-induced IMR90 and CAL51, 72hrs post transfection. Viability calculated versus the scrambled siRNA, per experiment. n=3 independent experiments for each cell line; *, p=0.0114 **, p=0.0016, for CAL51 and IMR90 respectively; unpaired t-test. **(l-m)** Comparison of BRAF (**l**) and CRAF (**m**) protein expression, between top and bottom aneuploidy quartiles of human cancer cell lines (n=168 and 166, for BRAF and CRAF, respectively). Data obtained from DepMap 22Q1 release[59]. Two-tailed Mann-Whitney test. **(o)** Correlation between CRAF activity and the drug response (AUC) of cancer cell lines to etoposide. Drug data obtained from the CTD^2 drug screen. Spearman correlation r=0.2874, p<0.0001. **(n)** Spearman's correlation of drug response (AUC) with CRAF activation between DNA damage inducers (DDR) and all other classes of drugs, from the CTD^2 drug screen. **, p=0.0028; Mann-Whitney test. **(p)** Drug sensitivity to 72hr treatment with a sub-lethal dose (200nM) of the CRAF inhibitor TAK632, in RPE1 clones (SS48, SS51 and SS111). Sub-lethal dose of CRAF inhibition had little (0%-5%) impact on cell viability. n=5 independent experiments. IC50 fold-change calculated relative to the DMSO-treated cells, per experiment; **, p=0.0086 (SS48); One-Sample t-test. Source data are provided as a Source Data file.

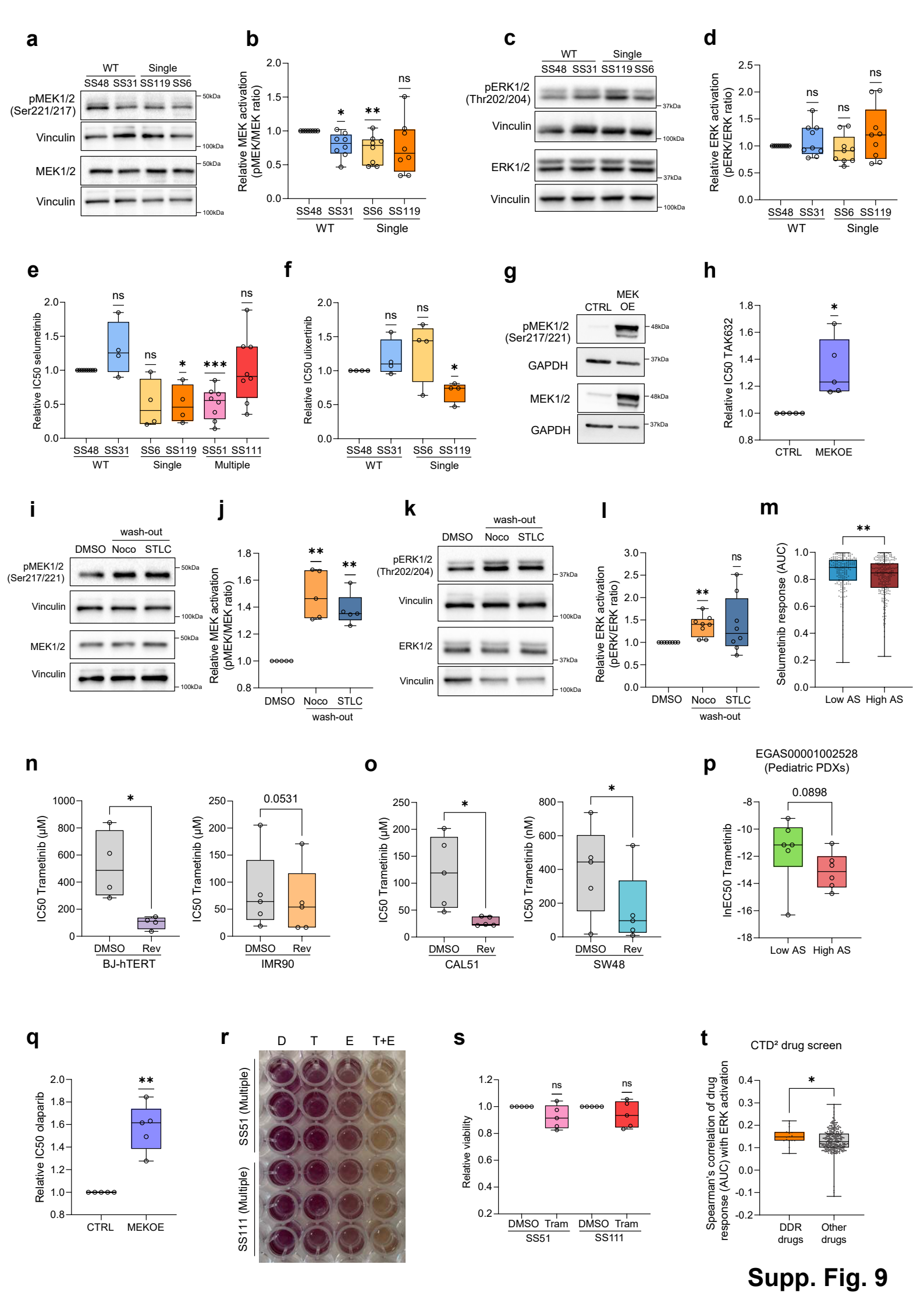
a
WT
Single
SS48 SS31 SS119 SS6
pMEK1/2 (Ser221/217)
Vinculin
MEK1/2
Vinculin
50kDa
100kDa
50kDa
100kDa
b
Relative MEK activation (pMEK/MEK ratio)
SS48 SS31 SS6 SS119
WT
Single
c
WT
Single
SS48 SS31 SS119 SS6
pERK1/2 (Thr202/204)
Vinculin
ERK1/2
Vinculin
37kDa
100kDa
37kDa
100kDa
d
Relative ERK activation (pERK/ERK ratio)
SS48 SS31 SS6 SS119
WT
Single
e
Relative IC50 selumetinib
SS48 SS31 SS6 SS119 SS51 SS111
WT
Single
Multiple
f
Relative IC50 ulixertinib
SS48 SS31 SS6 SS119
WT
Single
g
MEK
CTRL OE
pMEK1/2 (Ser217/221)
GAPDH
MEK1/2
GAPDH
48kDa
37kDa
48kDa
37kDa
h
Relative IC50 TAK632
CTRL MEKOE
i
wash-out
DMSO Noco STLC
pMEK1/2 (Ser217/221)
Vinculin
MEK1/2
Vinculin
50kDa
100kDa
50kDa
100kDa
j
Relative MEK activation (pMEK/MEK ratio)
DMSO Noco STLC
wash-out
k
wash-out
DMSO Noco STLC
pERK1/2 (Thr202/204)
Vinculin
ERK1/2
Vinculin
37kDa
100kDa
37kDa
100kDa
l
Relative ERK activation (pERK/ERK ratio)
DMSO Noco STLC
wash-out
m
Selumetinib response (AUC)
Low AS High AS
n
IC50 Trametinib (μM)
DMSO Rev
BJ-hTERT
IC50 Trametinib (μM)
0.0531
DMSO Rev
IMR90
o
IC50 Trametinib (μM)
DMSO Rev
CAL51
IC50 Trametinib (nM)
DMSO Rev
SW48
p
EGAS00001002528 (Pediatric PDXs)
0.0898
lnEC50 Trametinib
Low AS High AS
q
Relative IC50 olaparib
CTRL MEKOE
r
D T E T+E
SS51 (Multiple)
SS111 (Multiple)
s
Relative viability
DMSO Tram DMSO Tram
SS51 SS111
t
CTD² drug screen
Spearman's correlation of drug response (AUC) with ERK activation
DDR drugs Other drugs

Supp. Fig. 9

u

GSE235843 (PDAC, olaparib)

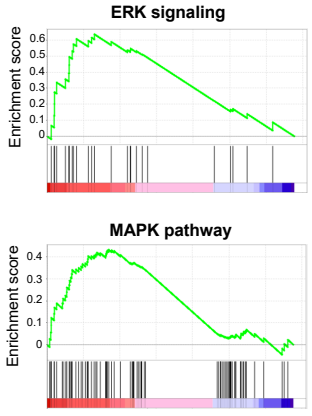

v

GSE173839 (Breast, olaparib/durvalumab)

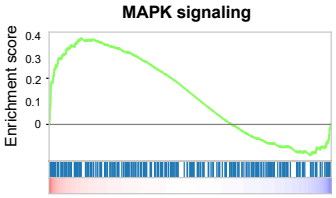

Supp. Fig. 9

Supplementary Figure 9: Increased sensitivity of aneuploid cells to MEK and ERK inhibition (related to Fig. 5)

(a) Western blot of pMEK1/2 (Ser221/217) and total MEK1/2 protein levels in pseudo-diploid and single-trisomy clones.**(b)** MEK1/2 activation (pMEK/MEK ratio) in each clone, relative to SS48 per experiment. n=8 independent experiments; *, p=0.0139 (SS31) and **, p=0.0085 (SS6); One-Sample t-test. **(c)** Western blot of pERK1/2 (Thr202/204) and total ERK1/2 protein levels in pseudo-diploid and single-trisomy clones **(d)** ERK1/2 activation (pERK/ERK ratio) in each clone relative to SS48, per experiment. n=9 independent experiments; One-Sample t-test **(e)** Drug sensitivity to 72hr drug treatment with MEK inhibitor selumetinib, in RPE1 clones. IC50 fold-change calculated relative to SS48, per experiment. n=4 (SS31, SS6, SS119) and n=6 (SS48, SS51, SS111) independent experiments; p=0.0675 (SS6), *, p=0.0377 (SS119) and ***, p=0.0007 (SS51); One-Sample t-test. **(f)** Drug sensitivity to 72hr drug treatment with the ERK inhibitor ulixertinib, between pseudo-diploid clones and single trisomy clones. IC50 fold-change calculated relative to SS48, per experiment. n=4 independent experiments; *, p=0.0264 (SS119); One-Sample t-test. **(g)** Western blot of pMEK1/2 (Ser221/217) and total MEK1/2 protein levels showing MEK overexpression in parental RPE1 cells. **(h)** Drug sensitivity to 72hrs treatment with CRAF inhibitor TAK632, in MEKOE RPE1 cells. IC50 fold change calculated relative to parental RPE1 cells, per experiment. n=5 independent experiments; *, p=0.027; One-sample t-test. **(i)** Western blot of pMEK1/2 and total MEK1/2 protein levels in aneuploidy-induced RPE1 cells using nocodazole or STLC. **(j)** MEK1/2 activation (pMEK/MEK ratio) in the aneuploidy-induced RPE1 cells, relative to DMSO control per experiment. n=5 independent experiments. **, p=0.0036 (nocodazole) and p=0.0020 (STLC); One Sample t-test. **(k)** Western blot of pERK1/2 and total ERK1/2 protein levels in aneuploidy-induced RPE1 cells using nocodazole or STLC**(l)** ERK activation (pERK/ERK ratio) in aneuploidy-induced RPE1 cells, relative to DMSO control per experiment. n=8 independent experiments. **, p=0.0029 (nocodazole); One Sample t-test. **(m)** Drug sensitivity to the MEK inhibitor selumetinib, between the top and bottom aneuploidy quartiles of human cancer cell lines (n=422). Data obtained from GDSC1 drug screen, DepMap 22Q1 release. **, p=0.0028; Two-tailed Mann-Whitney test. **(n-o)** Drug sensitivity of additional reversine-pulsed non-transformed (**n**, BJ-hTERT and IMR90) and cancer (**o**, CAL51 and SW48) cell lines to trametinib. (**n**) n=4 (BJ-hTERT) and n=5 (IMR90) independent experiment, per cell line; p=0.0531 (IMR90) and *, p=0.0443 (BJ-hTERT); paired t-test (**o**) n=5 independent experiments for each cell line; *, p=0.042 (CAL51) and p=0.0362 (SW48); paired t-test. **(p)** Drug response (lnEC50) of lowly and highly aneuploid pediatric PDXs to MEK inhibitor trametinib. Each dot represents a PDX tumor, n=6 tumors per group; p=0.0898, one-tailed Mann-Whitney t-test. **(q)** Drug sensitivity to 72hrs treatment with PARP inhibitor olaparib, in MEKOE RPE1 cells. IC50 fold-change calculated relative to parental RPE1 cells, per experiment. n=5 independent experiments; **, p=0.0036; One-sample t-test. **(r)** Representative image of the response (MTT assay) to the combination of a sub-lethal dose of trametinib with Etoposide. D, DMSO; T, trametinib 0.45nM; E, etoposide 2.5μM; T+E, combination trametinib and etoposide. **(s)** Viability following 72hrs treatment with a sub-lethal dose (0.45nM) of the MEK inhibitor trametinib, in highly-aneuploid RPE1 clones. n=5 independent experiments. Fold change in viability calculated relative to DMSO, per experiment; One-Sample t-test. **(t)** Spearman's correlation of drug response (AUC) with ERK activation between DNA damage inducers (DDR) and all other classes of drugs, from the CTD^2 drug screen. *, p=0.0409; one-tailed Mann-Whitney test. **(u)** GSEA of RAF/MEK/ERK(MAPK)-related signatures in pancreatic PDXs treated with olaparib (GSE235843), comparing the non-responsive to sensitive PDXs. Shown are enrichment plots for the Biocarta 'ERK pathway' (NES=1.69, p=0.0058) and 'MAPK pathway' (NES=1.44, p=0.0167). **(v)** GSEA of RAF/MEK/ERK (MAPK)-related signatures in breast tumors from patients treated with olaparib in combination with durvalumab (GSE173839), comparing the non-responsive to sensitive tumors. Shown are enrichment plots for the KEGG 'MAPK signaling pathway' gene set (NES=1.47, p=0.0011). Source data are provided as a Source Data file.

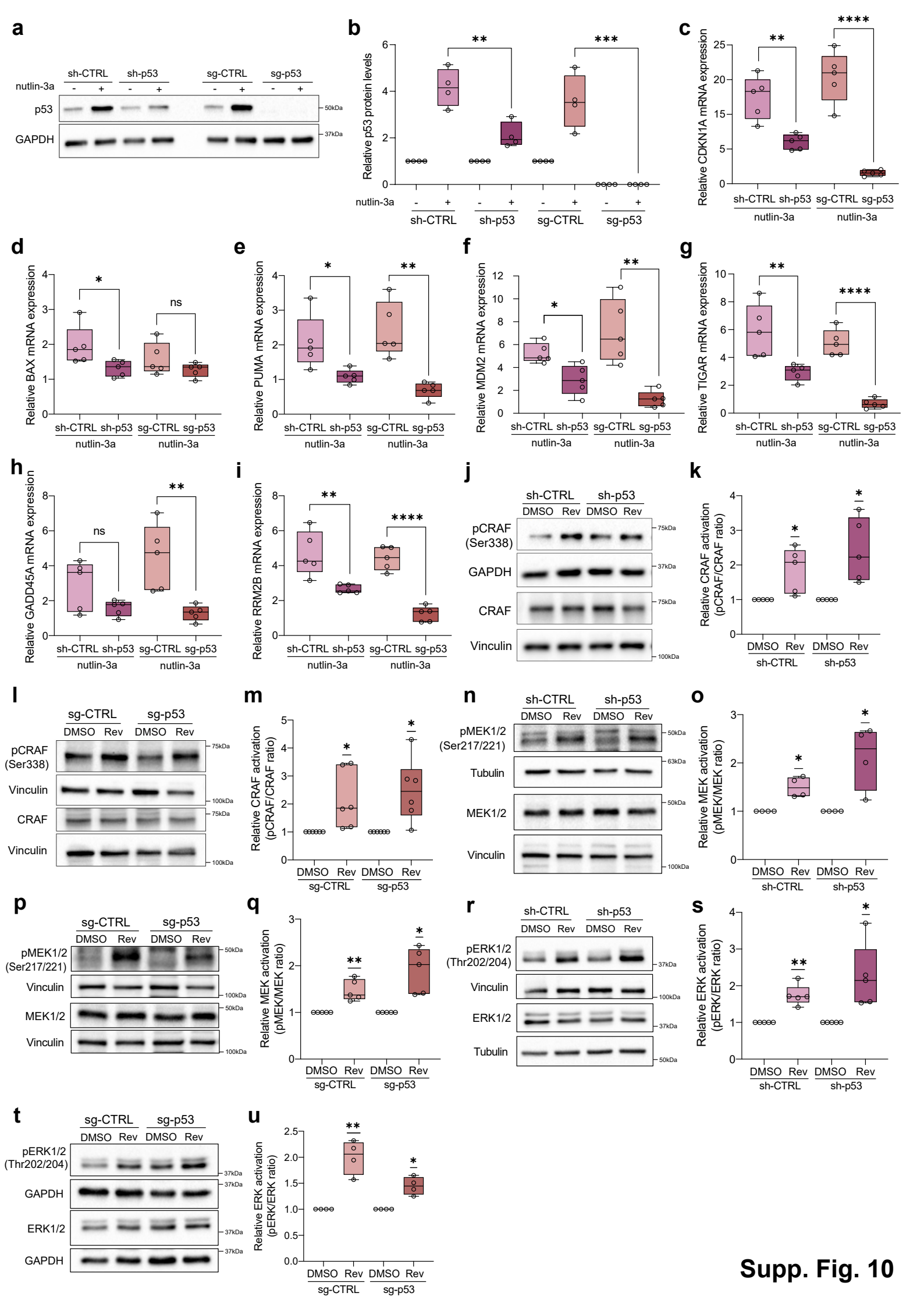
a
sh-CTRL
sh-p53
sg-CTRL
sg-p53
nutlin-3a
p53
GAPDH
50kDa
37kDa
b
Relative p53 protein levels
c
Relative CDKN1A mRNA expression
d
Relative BAX mRNA expression
e
Relative PUMA mRNA expression
f
Relative MDM2 mRNA expression
g
Relative TIGAR mRNA expression
h
Relative GADD45A mRNA expression
i
Relative RRM2B mRNA expression
j
pCRAF (Ser338)
GAPDH
CRAF
Vinculin
DMSO
Rev
k
Relative CRAF activation (pCRAF/CRAF ratio)
l
m
n
pMEK1/2 (Ser217/221)
Tubulin
MEK1/2
o
Relative MEK activation (pMEK/MEK ratio)
p
q
r
pERK1/2 (Thr202/204)
ERK1/2
s
Relative ERK activation (pERK/ERK ratio)
t
u
ns

Supp. Fig. 10

Supplementary Figure 10: RAF/MEK/ERK pathway activity is independent of p53 status in aneuploid RPE1 cells (related to Fig. 4 and Fig. 5)

(a) Western Blot showing p53 protein levels upon nutlin-3a stimulation in inducible *TP53*-KD and *TP53*-KO RPE1 cells. **(b)** Relative p53 protein levels upon nutlin-3a stimulation in inducible *TP53*-KD and *TP53*-KO RPE1-hTERT cells relative to their related controls. n=4 independent experiments. **, p=0.006 (*TP53*-KD) and ***, p=0.0009 (*TP53*-KO); two-tailed t-test. **(c-i)**: Downregulation of various p53 transcriptional targets (CDKN1A (**c**), BAX (**d**), PUMA (**e**), MDM2 (**f**), TIGAR (**g**), GADD45A (**h**), RRM2B (**i**)) following nutlin-3a stimulation in inducible *TP53*-KD and *TP53*-KO RPE1 cells, relative to their related controls. *, p<0.05, **, p<0.01, ***, p<0.001, ****, p<0.0001 for each comparison; two-tailed t-test. **(j)** Western blot of pCRAF and total CRAF protein levels in reversine-pulsed *TP53*-KD RPE1 cells **(k)** CRAF activation (pCRAF/CRAF ratio) in reversine-pulsed *TP53*-KD RPE1 parental cells, relative to the DMSO control per experiment. n=5 independent experiments. *, p=0.043 (sh-CTRL) and p=0.0227 (sh-p53); One Sample t-test. **(l)** Western blot of pCRAF and total CRAF protein levels in reversine-pulsed *TP53*-KO RPE1 cells **(m)** CRAF activation (pCRAF/CRAF ratio) in reversine-pulsed *TP53*-KO RPE1 cells, relative to DMSO control per experiment. n=6 independent experiments. *, p=0.043 (sg-CTRL) and p=0.0227 (sg-p53); One Sample t-test. **(n)** Western blot of pMEK1/2 and total MEK1/2 protein levels in reversine-pulsed *TP53*-KD RPE1 cells, **(o)** MEK1/2 activation (pMEK/MEK ratio) in the reversine-pulsed *TP53*-KD RPE1 cells, relative to DMSO control per experiment. n=4 independent experiments. *, p=0.0174 (sh-CTRL) and p=0.0424 (sh-p53); One Sample t-test. **(p)** Western blot of pMEK1/2 and total MEK1/2 protein levels in reversine-pulsed *TP53*-KO RPE1 cells **(q)** MEK1/2 activation (pMEK/MEK ratio) in reversine-pulsed *TP53*-KO RPE1 cells, relative to DMSO control, per experiment. n=5 independent experiments; **, p=0.0095 (sg-CTRL) and *, p=0.014 (sg-p53); One Sample t-test. **(r)** Western blot of pERK1/2 and total ERK1/2 protein levels in reversine-pulsed *TP53*-KD RPE1 cells. **(s)** ERK1/2 activation (pERK/ERK ratio) in the reversine-pulsed *TP53*-KD RPE1 cells, relative to the DMSO control, per experiment. n=5 independent experiments; **, p=0.0043 (sh-CTRL) and *, p=0.0337 (sh-p53); One Sample t-test. **(t)** Western blot of pERK1/2 and total ERK1/2 protein levels in reversine-pulsed *TP53*-KO RPE1 cells**(u)** ERK1/2 activation (pERK/ERK ratio) in the reversine-pulsed *TP53*-KO RPE1 cells, relative to DMSO control per experiment. n=4 independent experiments. **, p=0.0087 (sg-CTRL) and *, p=0.0136 (sg-p53); One Sample t-test. Source data are provided as a Source Data file.

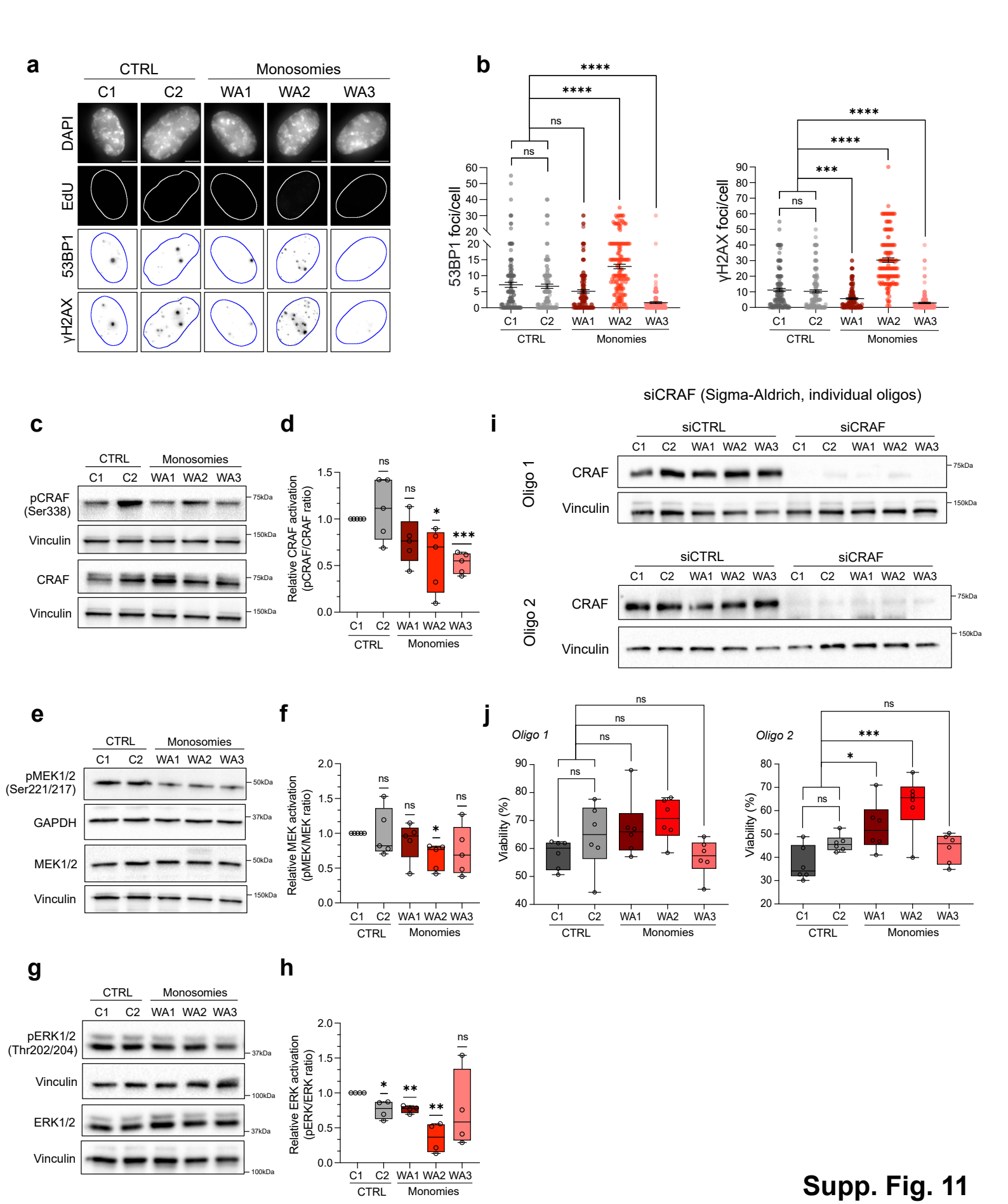
a
CTRL
Monosomies
C1
C2
WA1
WA2
WA3
DAPI
EdU
53BP1
γH2AX
b
53BP1 foci/cell
γH2AX foci/cell
ns
****
***
CTRL
Monomies
siCRAF (Sigma-Aldrich, individual oligos)
c
pCRAF (Ser338)
Vinculin
CRAF
75kDa
150kDa
d
Relative CRAF activation (pCRAF/CRAF ratio)
i
siCTRL
siCRAF
Oligo 1
Oligo 2
e
pMEK1/2 (Ser221/217)
GAPDH
MEK1/2
50kDa
37kDa
f
Relative MEK activation (pMEK/MEK ratio)
j
Oligo 1
Oligo 2
Viability (%)
g
pERK1/2 (Thr202/204)
ERK1/2
100kDa
h
Relative ERK activation (pERK/ERK ratio)

Supp. Fig. 11

Supplementary Figure 11: Monosomic RPE1 cells exhibit less DNA damage and are less dependent on the RAF/MEK/ERK pathway (related to Fig. 4 and Fig. 5)

(a) Immunofluorescence of 53BP1 and γH2AX foci in non-replicative (EdU-negative) pseudo-diploid *TP53*-null (C1 and C2) and monosomic (WA1, WA2 and WA3) clones. Scale bar, 5μm. **(b)** Comparison of 53BP1 (left) and γH2AX (right) foci between pseudo-diploid (C1 and C2) and monosomic (WA1, WA2 and WA3) clones. n=3 independent experiments, ~50 EdU negative nuclei analyzed per experiment. 53BP1: p=0.7844 (C1/C2, two-tailed Mann-Whitney test), and ****, p<0.0001 (CTRL/WA2 and CTRL/WA3), Kruskal-Wallis, Dunn's multiple comparison; γH2AX: p=0.2878 (C1/C2, two-tailed Mann-Whitney test), ***, p=0.0006 (CTRL/WA1), ****, p<0.0001 (CTRL/WA2 and CTRL/WA3); Kruskal-Wallis test, Dunn's multiple comparison. **(c-h)** Monosomic clones downregulate their RAF/MEK/ERK pathway activity. **(c)** Western blot of pCRAF (Ser338) and total CRAF protein levels, in controls and monosomic clones. **(d)** CRAF activation (pCRAF/CRAF ratio) relative to control C1 clone. *, p=0.0474 (WA2) and ***, p=0.0007 (WA3). One-sample t-test. **(e)** Western blot of pMEK1/2 (Ser221/217) and total MEK1/2 protein levels, in controls and monosomic clones. **(f)** MEK1/2 activation (pMEK/MEK ratio) relative to control C1 clone. *, p=0.0155 (WA2). One-sample t-test. **(g)** Western blot of pERK1/2 (Thr202/204) and total ERK1/2 protein levels, in controls and monosomic clones. **(h)** ERK1/2 activation (pERK/ERK ratio) relative to control C1 clone. *, p=0.0344 (C2) and **, p=0.0030 (WA1) and p=0.0093 (WA2). One-sample t-test **(i)** Western blot of total CRAF protein levels in controls and monosomic clones treated with individual siCRAF (or associated scrambled siRNA, Sigma-Aldrich) for 72hrs. **(j)** Viability in controls and monosomic clones, following siCRAF (or associated scrambled siRNA, Sigma-Aldrich), 72hr post transfection. Viability calculated versus scrambled siRNA treated cells, per experiment and per oligo. n=6 independent experiments for each oligo. No significant difference between the control clones (p=0.1276 and p=0.0685, for oligo 1 and oligo 2, respectively); two-tailed paired t-test. Oligo 2: *, p=0.0464 (CTRL/WA1) and ***, p=0.0002 (CTRL/WA2). One-way ANOVA, Tukey's multiple comparison. Source data are provided as a Source Data file.

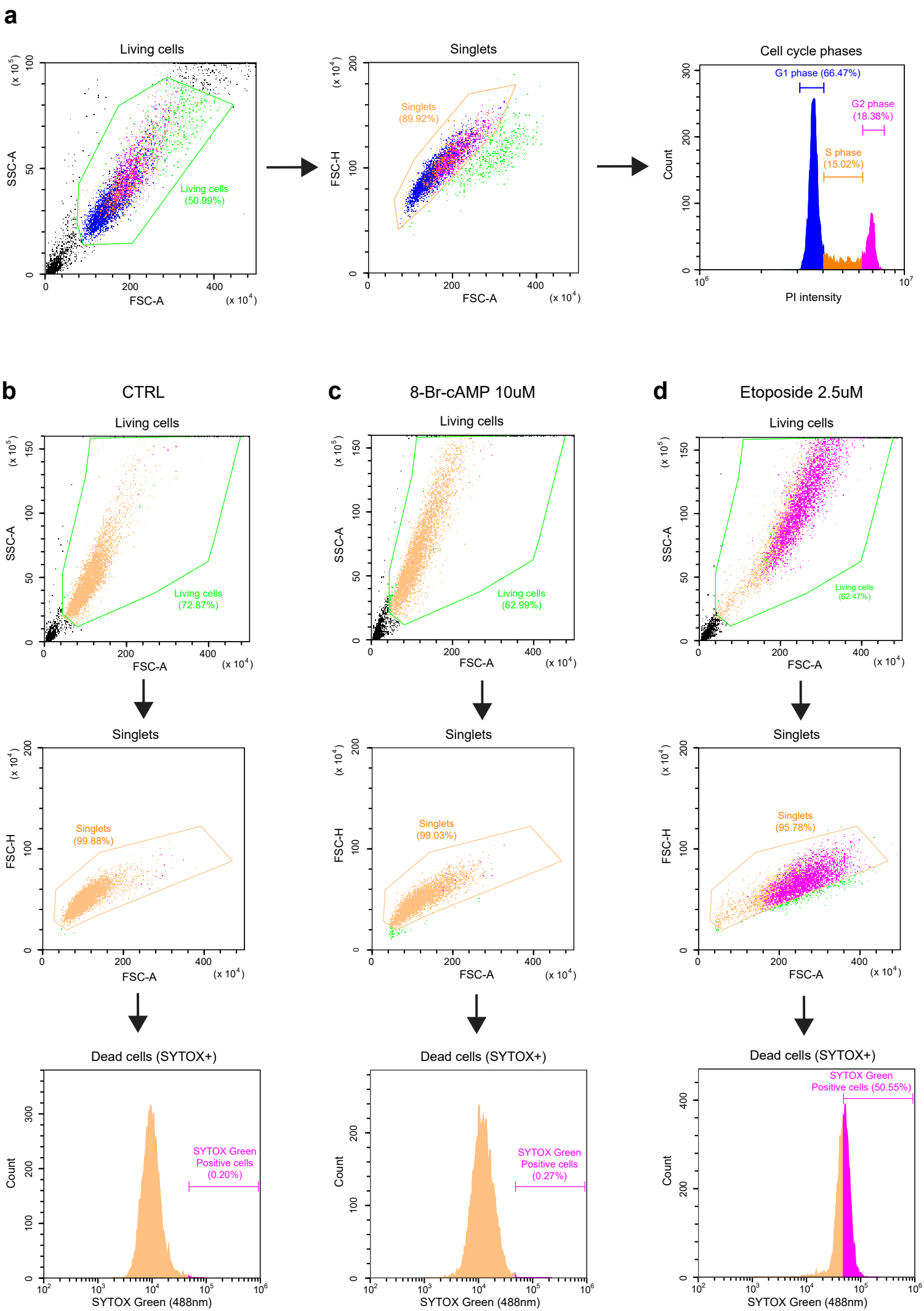
a
Living cells
SSC-A
FSC-A
Living cells
(50.99%)
Singlets
FSC-H
FSC-A
Singlets
(89.92%)
Cell cycle phases
Count
PI intensity
G1 phase (66.47%)
G2 phase
(18.38%)
S phase
(15.02%)
b
CTRL
Living cells
Living cells
(72.87%)
Singlets
Singlets
(99.88%)
Dead cells (SYTOX+)
SYTOX Green
Positive cells
(0.20%)
SYTOX Green (488nm)
c
8-Br-cAMP 10uM
Living cells
Living cells
(62.99%)
Singlets
Singlets
(99.03%)
Dead cells (SYTOX+)
SYTOX Green
Positive cells
(0.27%)
SYTOX Green (488nm)
d
Etoposide 2.5uM
Living cells
Living cells
(62.47%)
Singlets
Singlets
(95.78%)
Dead cells (SYTOX+)
SYTOX Green
Positive cells (50.55%)
SYTOX Green (488nm)

Supplementary Figure 12: Flow cytometry gating strategy

(**a**) Gating strategy applied to cell cycle analyses: definition of the living cells in All Events, then definition of the Singlets among the living cells, then definition of the cell cycle phases based on the PI intensity among the Singlets. (**b-d**) Gating strategy applied to cell death analyses using SYTOX Green, in control cells (**b**), cells treated with CRAF inhibitor 8-Br-cAMP 10uM (**c**) or DNA damage inducer Etoposide 2.5uM (**d**) as positive control, for 72hrs. Gating strategy consisted in the definition of the living cells in All Events, then definition of the Singlets among the living cells, then the definition of the dead cells based on the top50% SYTOX positive cells.

Supplementary Tables

Supplementary Table 1: Details of the High-Throughput Screening performed on the RPE1 isogenic model

Category	Parameter	Description
Assay	Type of assay	In vitro screen of a repurposing drug library (Corsello et al Nat Cancer 2020)
	Target	Drug Repurposing Library (Broad Institute; https://repo-hub.broadinstitute.org/repurposing#home) – contains multiple research, pre-clinical and clinical molecules many of which have an annotated protein target and/or mechanism of action
	Primary measurement	Cell viability following 72hrs treatment assessed using CellTiterGlo (Promega).
	Key reagents	Aneuploid RPE1-hTERT model – RPE1-SS48, RPE1-SS77, RPE1-SS6, RPE1-SS119, RPE1-SS51, RPE1-SS111. CellTiterGlo kit (Promega)
	Assay protocol	Screening performed following a modified version of the PRISM platform (Costello et al Nature Cancer 2020, doi: 10.1038/s43018-019-0018-6).
	Additional comments	
Library	Library size	5336 compounds
	Library composition	Multiple research, pre-clinical and clinical molecules, many of which have an annotated protein target and/ormechanism of action. (https://repo-hub.broadinstitute.org/repurposing-app)
	Source	Broad Institute (https://doi.org/10.1038/nm.4306)
	Additional comments	All compounds were tested in duplicates
Screen	Format	384-well plates, 300 cells/well
	Concentration(s) tested	2.5uM
	Plate controls	DMSO (negative control), Bortezomib (positive inhibitor control).
	Reagent/ compound dispensing system	Pre-plating using Beckman Coulter Labcyte Echo
	Detection instrument and software	Genedata Screener, Spotfire
	Assay validation/QC	“Active" compounds: mean of both replicates was equal, or less, than the activity threshold. "Inconclusive" compounds: if one of the two replicates was equal or less than the activity threshold, but the mean of both replicates was above the activity threshold. "Inactive" compounds: if neither of the replicates was equal or less than the activity threshold.
	Correction factors	None used
	Normalization	Following the equation as following: $Nx = CR + \frac{x - < cr >}{< sr > - < cr >}(SR - CR)$
	Additional comments	N is the normalized activity value, x is the measured raw signal of a well, <cr> is the median of the measured signal values of the Central Reference (DMSO control), <sr> is the median of the measured signal values of the Scale Reference (Inhibitor control), CR is the desired median normalized value for the Central Reference (0), and SR is the desired median normalized value for the Scale Reference (-100).
Post-HTS analysis	Hit criteria	Activity threshold: 3 time the standard deviation obtained in DMSO control.
	Hit rate	10.7% across all RPE1 clones
	Additional assay(s)	Concentration response confirmation assay was performed with 40 compounds testes at 8 concentrations, with 3-fold dilutions from 10uM to 4.5nM. EC50 values were calculated using Genedata Screener.
	Confirmation of hit purity and structure	Liquid chromatography-mass spectrometry (LC-MS). Information on purity and structure found at https://repo-hub.broadinstitute.org/repurposing-app.
	Additional comments	Assay Ready Plates (ARPs) made via the Labcyte Echo were used for the screen.

Supplementary Table 2: Reagents List

Antibodies			
Antibodies	**Source**	**Dilution**	**Identifier**
anti-Phospho-c-Raf (Ser338) (56A6)	Cell Signaling Technology	1:1000	Cat#9427 RRID:AB_2067317
anti-c-Raf	BD Biotechnologies	1:1000	Cat#610152 RRID:AB_397553
	Cell Signaling Technology	1:1000	Cat#9422 RRID:AB_390808
anti-Phospho-MEK1/2 (Ser217/221)	Cell Signaling Technology	1:1000	Cat#9121 RRID:AB_331648
anti- MEK1/2	Cell Signaling Technology	1:1000	Cat#9122 RRID:AB_823567
anti-Phospho-ERK1/2 (Thr202/Tyr204) XP®	Cell Signaling Technology	1:1000	Cat#4370 RRID:AB_2315112
anti- ERK1/2	Santa-Cruz Biotechnologies	1:1000	Cat#sc-514302 RRID:AB_2571739
anti-Phospho-Histone H2A.X (Ser139)	Cell Signaling Technology	1:1000	Cat#9718 RRID:AB_2118009
	Millipore	1:1000	Cat#05-636 RRID:AB_309864
anti-53BP1	Abcam	1:1000	Cat#ab175933 RRID:AB_2890610
anti-p53	Cell Signaling Technology	1:1000	Cat#9282 RRID:AB_331476
	Santa-Cruz	1:1000	Cat#sc-393031 RRID:AB_3083496
anti-p21	Cell Signaling Technology	1:1000	Cat#2947 RRID :AB_823586
anti-GAPDH	Cell Signaling Technology	1:1000	Cat#2118 RRID:AB_561053
anti-Vinculin	Sigma-Aldrich	1:2000	Cat#V9131 RRID:AB_477629
anti-Tubulin	Sigma-Aldrich	1:2000	Cat#T9026 RRID:AB_477593
HRP-conjugated Goat anti-mouse IgG	Jackson ImmunoResearch Labs	1:10000	Cat#115-035-003 RRID:AB_10015289
HRP-conjugated Goat anti-rabbit IgG	Jackson ImmunoResearch Labs	1:10000	Cat#111-035-003 RRID:AB_2313567
Alexa Fluor® 488 conjugated IgG	Cell Signaling Technology	1:1000	Cat#4408 RRID:AB_10694704
	Jackson ImmunoResearch Labs	1:400	Cat#711-545-152 RRID:AB_2313584
Alexa Fluor® 555 conjugated IgG	Cell Signaling Technology	1:1000	Cat#4409 RRID:AB_1904022
Alexa-Cy3 conjugated IgG	Jackson ImmunoResearch Labs	1:400	Cat#715-165-150 RRID:AB_2340813

Drugs		
Drugs	**Source**	**Identifier**
Reversine	MedChemExpress	Cat#HY-14711
Thymidine	Sigma-Aldrich	Cat#T1895
Etoposide	Cayman Chemicals	Cat#12092
Olaparib	Cayman Chemicals	Cat#10621
Nutlin-3a	SelleckChem	Cat#S1061
TAK632	Cayman Chemicals	Cat#16285
8-Br-cAMP	Sigma-Aldrich	Cat#B7880
PLX7904	Cayman Chemicals	Cat#18298
Selumetinib	SelleckChem	Cat#S1008
Trametinib	Cayman Chemicals	Cat#16292
Ulixertinib	Cayman Chemicals	Cat#18298

Oligonucleotides		
Oligonucleotides	**Source**	**Sequence**
ON-TARGETplus SMARTpool® Non-targeting	Dharmacon	Cat#D-001810-10-05
ON-TARGETplus SMARTpool® CRAF	Dharmacon	Cat#L-003601-00-0005
siRNA targeting CRAF (oligo 1)	Sigma-Aldrich	Cat#SASI_Hs01_00174876
siRNA targeting CRAF (oligo 2)	Sigma-Aldrich	Cat#SASI_Hs01_00174878
siRNA targeting BRAF (oligo 1)	Sigma-Aldrich	Cat#SASI_Hs01_00107703
siRNA targeting BRAF (oligo 2)	Sigma-Aldrich	Cat#SASI_Hs01_00107705
Lentiviral packaging vectors	Addgene	pMDL #12251
		pRev #12253
		pMDG #187440
Scramble shRNA	This paper	CCGGCCTAAGGTTAAGTCGCCCTCGCTCGAGC GAGGGCGACTTAACCTTAGGTTTTTG
TP53 shRNA	This paper	CCGGGTCCAGATGAAGCTCCCAGAACTCGAGT TCTGGGAGCTTCATCTGGACTTTTTG
pHAGE-MAP2K1 (MEK-OE vector)	Addgene	#116757
GADD45A qRT-PCR primers	This paper	F: 5’-TGCGAGAACGACATCAACAT-3’
		R: 5’-GCAGGATCCTTCCATTGAGA-3’
CDK1A qRT-PCR primers	This paper	F: 5’-GGAAGACCATGTGGACCTGT-3’
		R: 5’-GGATTAGGGCTTCTTCTTGG-3’
RRM2B qRT-PCR primers	This paper	F: 5’-CCTTGCGATGGATAGCAGATAG-3’
		R: 5’-GCCAGAATATAGCAGCAAAAGATC-3’
BAX qRT-PCR primers	This paper	F: 5’-TCTGACGGCAACTTCAACTG-3’
		R: 5’-TTGAGGAGTCTCACCCAACC-3’
PUMA qRT-PCR primers	This paper	F: 5’-GTCCCCTGCCAGATTTGTG-3’
		R: 5’-AGAGGCCGCACACTG-3’
MDM2 qRT-PCR primers	This paper	F: 5’-GTGGCGTTTTCTTTGTCGTT-3’
		R: 5’-GGTGGGAGTGATCAAAAAGA-3’
TIGAR qRT-PCR primers	This paper	F: 5’-CGGCATGGAGAAACAAGATT-3’
		R: 5’-CATGGTCTGCTTTGTCCTCA-3’
BRAF qRT-PCR primers	This paper	F: 5’-ATGTTGAATGTGACAGCACC-3’
		R: 5’-CTCACACCACTGGGTAACAA-3’
GAPDH qRT-PCR primers	This paper	F: 5’-GAGTCAACGGATTTGGTCGT-3’
		R: 5’-GACAAGCTTCCCGTTCTCAG-3’

Critical commercial assays		
Reagents	**Source**	**Identifier**
MTT (Thiazolyl Blue Tetrazolium Bromide)	Sigma-Aldrich	Cat#M2128
CellTiterGlo®	Promega	Cat#G9241
Bio-TRI®	Bio-Lab	Cat#959758027100
GoScript™ Reverse Transcription System	Promega	Cat#A5000
Lipofectamine RNAiMAX®	Invitrogen	Cat#13778-075
TransIT-LT1®	Mirus	Cat#MIR2300
Dharmafect1	Dharmacon	Cat#T-2001-02
TURBO DNA-free™ Kit	Invitrogen	Cat#AM1907
PowerSYBR™ Green PCR Master Mix	Invitrogen	Cat#4368702
NP-40 lysis buffer	Home-made	N/A
Bradford Protein Assay Dye Reagent Concentrate	Bio-Rad	Cat#5000006
Immobilon® Crescendo	Millipore	Cat#WBLUR0500
SYTOX™ Green Ready Flow™ Reagent	Invitrogen	Cat#R37168
EZClick™ Global RNA Synthesis Assay Kit (FACS/Microscopy), Red Fluorescence	BioVision	Cat#K718
Protease inhibitor cocktail	Sigma-Aldrich	Cat#P8340
Phosphatase inhibitor cocktail	Sigma-Aldrich	Cat#P0044